DET NORSKE VIDENSKAPS-AKADEMI I OSLO

GEOFYSISKE PUBLIKASJONER

GEOPHYSICA NORVEGICA

VOL. XXVIII. No. 6 JULY 1972

Aksel Wiin-Nielsen

Simulations of the Annual Variation of the Zonally Averaged State of the Atmosphere

OSLO 1972
UNIVERSITETSFORLAGET

G E O F Y S I S K E P U B L I K A S J O N E R
G E O P H Y S I C A N O R V E G I C A

VOL. XXVIII. NO. 6

SIMULATIONS OF THE ANNUAL VARIATION OF THE ZONALLY AVERAGED STATE OF THE ATMOSPHERE

By

Aksel Wiin-Nielsen

FREMLAGT I VIDENSKAPS-AKADEMIETS MØTE DEN 4. FEBRUAR 1972 AV ELIASSEN

Summary. A two-level, quasi-geostrophic model for the zonally averaged state of the atmosphere containing diabatic heating, internal as well as boundary layer friction, and exchange processes for the transport of quasi-geostrophic potential vorticity and sensible heat, has been integrated for the basic period of a year using expansion in Legendre functions in space and trigonometric functions in time.

The model is more realistic than earlier models mainly in the specification of the diabatic heating, which now includes crude parameterizations of small-scale convection and latent heat release in addition to short- and long-wave radiation. The heat balance at the surface is obtained through the processes of short- and long-wave radiation, small-scale convection, evaporation and subsurface conduction.

The results of several integrations show that the model is capable of a more realistic description of the annual variation of the energetics of the atmosphere, and, especially, that the amplitude of the annual variation is greatly reduced as compared with the earlier model which contained radiation processes only.

In addition to the energetics of the model, an analysis of the zonal averages of temperature, winds, vertical velocity, momentum and heat transports, the diabatic heating and the surface temperature is made for one experiment. Each of these quantities, computed by the model experiment, show at least a good qualitative agreement with results based on observations.

1. Introduction. The purpose of this paper is to describe an improved simulation of the annual variation of the atmospheric energetics. It is pertinent to start with a short review of the earlier work on this subject. Through diagnostic studies of the annual variation of atmospheric energetics (Wiin-Nielsen, 1967) it was shown, applying Fourier analysis to the time series, that the maximum generation of available potential energy occurs late in the year, while the maximum dissipation of kinetic energy takes place early in the year. Similar results have been obtained by Kung and Soong (1969) considering the kinetic energy through the seasons. The first attempts to simulate the annual variation of atmospheric energetics (Wiin-Nielsen, 1968 a, 1970) were simply directed at reproducing, from theoretical models, the typical time lag between the generation of available potential energy and the dissipation of kinetic energy in the zonally averaged fields. As it turns out, the time lag can be reproduced with an extremely simple model which simulates the dynamics of the atmosphere in a very crude way as seen by the first investigation of the problem by Wiin-Nielsen (1968a).

As an outgrowth of the investigations mentioned above, it has appeared that it may be possible to obtain a somewhat more detailed simulation of the annual variation of the zonally averaged state of the atmosphere including some aspects of the seasonal variation of the energetics of this atmospheric flow. It has recently been demonstrated (Saltzman (1968)) that it is possible to obtain solutions for the zonally averaged variables (the axially-symmetric component) in the steady-state case which supposedly corresponds to the time-average over an ensemble of similar states. The present investigation is to a large extent a generalization of such investigations to the case where variations in time through the year are permitted.

A simulation of the annual variations using models with the same time and space resolution as is presently employed to simulate the general circulation by extended time integration has not been attempted in the past, presumably because of too excessive demands on computer time and perhaps because of numerical difficulties. However, integrations covering many years of real time have been carried out by Kraus and Lorenz (1966) using a system with relatively few degrees of freedom. While much can be learned from such a system, it is nevertheless cumbersome to model the geometry correctly, to include the interaction among waves, and to represent local processes in a low order system.

In the previous investigations by the author it was decided to predict the zonal averages of the various parameters in the model and to include, if possible, the important interactions between the eddies and the zonally averaged parameters by a suitable parameterization. The major interactions between the eddies and the zonal average is the transport of heat and momentum by the eddies influencing directly the zonally averaged temperature field and the zonally averaged wind field, respectively. The problem of relating the meridional transports of heat and momentum to zonally averaged parameters has been treated in an earlier paper (Wiin-Nielsen and Sela, 1971) where it was shown that the meridional transports of sensible heat and quasi-geostrophic potential vorticity to a first degree of approximation can be treated as exchange processes. The theoretical foundation for such a treatment has been given by Green (1970) based upon a detailed analysis of the behaviour of transient atmospheric waves.

As shown by Green (loc. cit.) it is possible to parameterize the convergence of the momentum transport indirectly from the assumptions concerning the transports of sensible heat and quasi-geostrophic potential vorticity.

The procedure outlined above for the parameterization of the various meridional transports was used by Sela and Wiin-Nielsen (1971) to simulate the annual variation of atmospheric energetics using a two level, quasi-geostrophic model. The zonally averaged equations for this model were integrated for a period of a few years starting from an isothermal atmosphere at rest. The main discrepancy between the behaviour of the numerical solution and the atmospheric flow in this experiment was that the model predicted a too large variation of almost all energy parameters, but that the observed phase relationships were predicted in an essentially correct manner. However, this experiment as well as the integration of a case containing the same physical processes, but a simpler geometry (β-plane approximation) (Wiin-Nielsen, 1971) provided an excellent test of the validity of the approach to the problem, and it was possible to show that the main reason for the difference between the predicted and observed flow was the simplicity of the heating mechanism in the model. The two experiments were successful in predicting many of the features of the observed circulation and its annual variation in a qualitatively correct way including the correct directions of the energy flow through the atmosphere.

The heating in the experiments which have been reported up to the present time (Wiin-Nielsen, 1968a, 1970, 1971 and Sela and Wiin-Nielsen, 1971) has been of a Newtonian form, where the coefficient in the heating function was determined empirically, and where the required equilibrium temperature was calculated from a very elementary radiational equilibrium consideration described in detail by Wiin-Nielsen (1970). In addition to considerations of radiation it is naturally also necessary to consider the interaction between the atmosphere and the underlying surface in the form of exchange of heat by conduction, convection and evaporation, and to model the net heating of the atmosphere by these processes. The main purpose of the present paper is to describe how the heating has been included in the model and to show the results of several experiments with the improved model.

It should be stressed that the present investigation deals with the zonally averaged state of the atmosphere. In order to predict the annual variation of the zonally averaged parameters it is necessary to specify the exchange processes between the eddies and the zonal mean. We have been able to do this by empirical methods but it is then implicitly assumed that the transport of the eddies is as implied by the specification. The present model is therefore too simple to discuss the various possibilities which exist for Hadley and Rossby regimes in the atmospheric flow.

2. The Model. The basic model to be used in these experiments is the same as before, i.e. the quasi-geostrophic, two-level model. The two equations for the model are:

$$\frac{\partial Q_1}{\partial t} + \nabla \cdot (Q_1 \vec{v}_1) = -\lambda^2 \frac{R}{2f_o} \frac{1}{Cp} H_2 - \frac{g}{P} \vec{k} \cdot \nabla x \vec{\tau}_2 \tag{2.1}$$

$$\frac{\partial Q_3}{\partial t} + \nabla \cdot (Q_3 \vec{v}_3) = +\lambda^2 \frac{R}{2f_o} \frac{1}{Cp} H_2 + \frac{g}{P} \vec{k} \cdot \nabla x \vec{\tau}_2 - \frac{g}{P} \vec{k} \cdot \nabla x \vec{\tau}_4 \tag{2.2}$$

where

$$Q_1 = f + \zeta_1 - \lambda^2 \psi_T \tag{2.3}$$

$$Q_3 = f + \zeta_3 + \lambda^2 \psi_T \tag{2.4}$$

are the quasi-geostrophic, potential vorticities at level 1 (25 cb) and level 3 (75 cb), respectively, f is the Coriolis parameter, $\lambda^2 = 2f_o^2/(\sigma_2 P^2)$, where f_o is a standard value of f, P = 50 cb, and $\sigma_2 = -(\alpha_2/\theta_2)\,(\partial\theta/\partial P)_2$ is the stability parameter at level 2 (50 cb), and

$$\psi_T = \tfrac{1}{2}(\psi_1 - \psi_3) \tag{2.5}$$

is the thermal stream function. The remaining symbols in (2.1) and (2.2) are: R, the gas constant, C_p the specific heat for constant pressure, g the acceleration of gravity, $\vec{\tau}_2$ and $\vec{\tau}_4$ the stress vectors at levels 2 and 4, respectively, and $\vec{k}$ a vertical unit vector. The two frictional terms will be calculated in the following way. We assume that

$$\vec{\tau}_2 = +\nu\varrho \left(\frac{\partial \vec{v}}{\partial z}\right)_2 \tag{2.6}$$

Converting to pressure as the vertical coordinate, taking finite differences over a layer of P = 50 cb we get

$$\frac{g}{P} \vec{k} \cdot \nabla x \vec{\tau}_2 = -2A\zeta_T \tag{2.7}$$

where

$$A = \frac{g^2 \nu}{R^2 T_2^2} \tag{2.8}$$

and $$\zeta_T = \tfrac{1}{2}(\zeta_1 - \zeta_3) \tag{2.9}$$

Regarding the surface stress we assume that

$$\vec{\tau}_4 = -\varrho_4 C_d V_4 \vec{v}_4 \tag{2.10}$$

where ϱ_4 is the density, C_d the drag coefficient, and V_4 a standard value of the surface wind. Using (2.10) we find, considering the coefficient as a constant, that

$$\frac{g}{P}\vec{k} \cdot \nabla x \vec{\tau}_4 = -\varepsilon\zeta_4 \tag{2.11}$$

where

$$\varepsilon = \frac{g}{P} Cd\, \varrho_4 V_4 \tag{2.12}$$

In the previous experiments we have calculated ζ_4, the relative vorticity at level 4 (100 cb), using a linear extrapolation from the levels 1 and 3. As shown by Sela and Wiin-Nielsen (1971) there are certain undesirable features connected with this procedure because there is no guarantee that the dissipation of the kinetic energy will be positive. In this paper we shall use the assumption that

$$\zeta_4 = \tfrac{1}{2}\zeta_3 \tag{2.13}$$

which results in a positive dissipation of kinetic energy.

In specifying the heating H_2 in the model we have followed the procedure outlined by Saltzman (1968) to a very large extent, including adopting the numerical values of the empirical constants given by him. It will therefore suffice to summarize his procedure by referring to Table 1, where we have reproduced the functional form for the heat transfer across the surface interface, $HT_s = \sum_{n=1}^{5} HT_s^{(n)}$ and the heat transfer for the net heating of the atmosphere $HT_a = \sum_{n=1}^{5} HT_a^{(n)}$. We note that

$$H_2 = \frac{g}{p_o} HT_a \tag{2.14}$$

The symbols appearing in Table 1 are as follows:

R_o = intensity of solar radiation at top of atmosphere
T_D = subsurface temperature
T_s = surface temperature
T_2 = atmospheric temperature (50 cb)
X = opacity of the atmosphere to solar radiation
r_s = albedo of surface

r_a = albedo of atmosphere
σ_B = Stefan-Boltzman constant
N_1, N_2 = factors for downward and upward effective blackbody long-wave radiation from atmosphere.
Γ = long-wave absorptivity of atmosphere
w = water availability
k = factor proportional to the conductive capacity of the surface medium
b, c, e, f = empirical constants

The physical variables in this set are the first four listed above of which R_o is given as a function of latitude and time of the year (Wiin-Nielsen, 1970). T_D can be estimated in various ways. In the present investigation we have adopted as T_D the zonal average of the sea surface temperatures given month by month for the Pacific Ocean by Clark (1967).

Table I

n	$HT_s^{(n)}$	Parameterization
1	Short-wave solar radiation	$(1 - x)\,(1 - r_a)\,(1 - r_s)\,R_o$
2	Long-wave radiation	$\sigma_B\,(N_1 T_2^4 - T_s^4)$
3	Small-scale convection	$-\,[b(T_s - T_2) + c]$
4	Evaporation and condensation	$w\,[e\,HT_s^{(3)} + f]$
5	Subsurface conduction	$-\,K(T_s - T_D)$
n	$HT_a^{(n)}$	Parameterization
1	Short-wave solar radiation	$X(1 - r_a)R_o$
2	Long-wave radiation	$\sigma_B[\Gamma T_s^4 - (N_1 + N_2)T_2^4]$
3	Small-scale convection	$-\,HT_s^{(3)}$
4	Latent heat release	$-\int_o^1 HT_s^{(4)}\,d\mu$

These temperatures cover the latitude belt 20°N to 55°N. An extrapolation to cover the region between equator and pole was performed, guided by the curve for T_D given by Saltzman (1968) for the annual average for the Atlantic Ocean. The resulting field of temperatures is given in Table II as a function of latitude and time.

The calculation of the heating H_2 in (2.14) may be carried out in the following way. The expression

$$HT_a = \sum_{n=1}^{4} HT_a^{(n)} \tag{2.15}$$

contains two unknown fields T_2 and T_s. We may eliminate one of these fields, for example T_s, using the condition

$$HT_s = \sum_{n=1}^{5} HT_s^{(n)} = 0 \tag{2.16}$$

expressing equilibrium at the interface between the atmosphere and the underlying surface. The resulting expression for H_2 depends then only on the field T_2, which can be expressed in terms of the dependent variable ψ_T appearing in (2.5) through the relation:

$$\psi_T = \frac{R}{2f_o} T_2 \tag{2.17}$$

The equations which are integrated are the zonally averaged equations obtained from (2.1) and (2.2). We get using (2.7) and (2.11):

$$\frac{\partial Q_{1z}}{\partial t} + \frac{1}{a\cos\varphi}\frac{\partial (Q_1 v_1)_z \cos\varphi}{\partial\varphi} = -\lambda^2 \frac{R}{2f_o}\frac{1}{Cp} H_{2z} - 2A\zeta_{Tz} \tag{2.18}$$

$$\frac{\partial Q_{3z}}{\partial t} + \frac{1}{a\cos\varphi}\frac{\partial (Q_3 v_3)_z \cos\varphi}{\partial\varphi} = +\lambda^2 \frac{R}{2f_o}\frac{1}{Cp} H_{2z} + 2A\zeta_{Tz} - \frac{\varepsilon}{2}\zeta_{3z} \tag{2.19}$$

In order to close the system (2.18), (2.19) we introduce the approximations

$$(Q_1 v_1)_z = -K_1 \frac{\partial Q_{1z}}{a\partial\varphi} \tag{2.20}$$

$$(Q_3 v_3)_z = -K_3 \frac{\partial Q_{3z}}{a\partial\varphi} \tag{2.21}$$

The validity of (2.20) and (2.21) was discussed by Wiin-Nielsen and Sela (1971). They showed that the meridional transport of quasi-geostrophic, potential vorticity is negative (toward the south) in the troposphere above the planetary boundary layer. Since the gradient of the zonally averaged potential vorticity is positive almost everywhere, they showed that K_1 and K_3 were positive. The dependences of K_1 and K_3 on latitude were displayed, and the distributions $K_1 = K_1(\varphi)$ and $K_3 = K_3(\varphi)$ were used for a numerical integration of the model equations described by Sela and Wiin-Nielsen (1971). The major difference between that calculation and the one to be described here is in the determination of the heating H_{2z} which in the former integration was based upon radiational considerations while we have now included additional processes as seen in Table I.

Since one of the purposes of the present calculation was to investigate a relatively large number of cases it was important to have an efficient way of integration of (2.20) and (2.21). While the equations can be integrated using a normal finite difference method as shown by Sela and Wiin-Nielsen (1971), we are mainly interested in the annual averages and the gross aspects of the variation through the year. It was therefore decided to use a method of integration similar to the one employed by Wiin-Nielsen (1970) in which the basic variables were expressed as truncated series of Legendre functions having coefficients which depend upon

Table II

T_D, ^{0}K.

φ \ t	Jan.	Feb.	March	Apr.	May	June	July	Aug.	Sept.	Oct.	Nov.	Dec.
90	273.00	273.00	273.00	273.00	273.00	273.00	273.00	273.00	273.00	273.00	273.00	273.00
80	273.61	273.54	273.45	273.63	274.09	274.61	275.30	275.22	274.89	274.59	274.32	273.93
70	275.37	274.87	274.62	275.11	276.42	277.92	279.93	279.95	279.06	278.11	277.19	276.03
60	277.25	276.59	276.28	276.87	278.59	280.62	283.54	284.34	283.30	281.79	280.04	278.28
50	278.68	278.23	278.08	278.31	279.42	281.06	283.49	286.06	285.72	283.91	281.51	279.77
40	285.14	284.22	284.02	284.75	285.72	287.65	290.73	293.52	293.16	291.09	288.58	286.56
30	292.33	291.56	291.43	292.00	293.45	295.29	297.14	298.12	298.25	297.13	295.55	293.89
20	297.50	297.07	297.00	297.45	298.22	299.17	299.87	300.37	300.43	300.15	299.39	298.43
10	300.77	300.60	300.53	300.78	300.95	301.24	301.26	301.98	301.84	301.89	301.56	301.26
0	301.86	301.77	301.70	301.89	301.86	301.93	301.73	302.51	302.31	302.47	302.30	302.21

time only. The variation in time was taken into account by expressing the time variation of the coefficients as a truncated Fourier series in time having one year as the basic period and including, in addition to the annual average, the first three Fourier components of the annual variation.

In order to use the integration procedure outlined above, it is clearly an advantage to assume that K_1 and K_3 are constants. In the previous integration by Sela and Wiin-Nielsen (1971), K_1 and K_3 were both functions of latitude. However, in this investigation we shall keep K_1 and K_3 constant. We cannot expect to be able to reproduce the details of the meridional distributions under these circumstances.

It is finally convenient and necessary to make the expression for H_{2z} linear in the temperatures. This is done in the same way as previously by approximating T^4 in the following form:

$$T_4 = 4\,T_o^3 T - 3\,T_o^4,\ T_o = 273^\circ\text{K} \tag{2.22}$$

Since the general procedure is exactly the same as outlined by Wiin-Nielsen (1970), we shall abstain from giving the detailed derivation of the equations for the coefficients in the expansions in Legendre functions and the Fourier series. However, it should be mentioned that the series of Legendre functions was restricted to even functions, and that the maximum degree allowed was 6. The expansion in Fourier series was restricted to the annual mean plus the first three Fourier components having periods of 12, 6 and 4 months.

The dependent variables which are predicted directly by the model equations are the stream-functions ψ_1 and ψ_3. From these variables we may compute a number of derived quantities. In the present calculation we computed the zonal winds $U_{1z}(\mu, t)$[1] and $U_{3z}(\mu, t)$ and the mid-tropospheric temperature $T_{2z}(\mu, t)$. Due to the model approximations it is also possible to compute such quantities as the transport of heat. Using the model approximation

[1] $\mu = \sin\varphi$.

$$(Tv)_z = - K_H \frac{\partial T_z}{a \partial \varphi} \tag{2.23}$$

and the thermal wind equation it turns out that we may write the heat transport across a given latitude in a layer of thickness Δp in the form

$$HT(t, \mu) = \frac{\Delta p}{g} c_p \frac{2f_o}{R} K_H 2\pi a \sqrt{1 - \mu^2}\, U_T(t, \mu) \tag{2.24}$$

where

$$U_T = \tfrac{1}{2}(U_1 - U_3) \tag{2.25}$$

Using the parameterization of the momentum transport developed by Wiin-Nielsen and Sela (1971), it is furthermore possible to compute the angular momentum transport at the upper and lower levels as a function of latitude and time. Regarding the energetics of the model it is possible to compute the following quantities:

A_z, zonal available potential energy
K_z, zonal kinetic energy
$G(A_z)$, generation of zonal available potential energy
$C(A_z, A_E)$, conversion from zonal to eddy available potential energy
$C(A_z, K_z)$, comversion from zonal available potential energy to zonal kinetic energy
$C(K_E, K_z)$, conversion from eddy to zonal kinetic energy
$D(K_z)$,dissipation of zonal kinetic energy

The formulas for the various quantities are given by Wiin-Nielsen (1970) and Sela and Wiin-Nielsen (1971).

3. Results. It is naturally possible to perform a large number of experiments varying the many parameters entering the model equations. Some of these experiments are of interest because they are close to observed atmospheric conditions while others will be far removed from the observed state of the atmosphere. We shall use the energetics of the model experiments to give us a first impression of the behaviour of the model atmosphere. Based upon the comparison between the energetics of the experiment and of the real atmosphere we may select to analyse some of the experiments in greater detail.

From the study of the amounts of atmospheric energy by Wiin-Nielsen (1967) we have an estimate of the annual variation of A_z and K_z. In order to characterize the annual variation in a relatively easy manner we have included only the annual mean and the first Fourier component, making it possible to give the maximum and minimum and the time at which they occur. This information taken from Wiin-Nielsen (1967) and based on observations is given in Table III, which will be used for comparative purposes.

Table III

	Amount, kjm^{-2}	Time, days
A_z, max	4360	20
A_z, min	1968	200
K_z, max	1468	24
K_z, min	196	204

We shall next describe a number of experiments which have been performed using the model described in section 2. In this series of experiments we have used the following set of numerical values for the parameters:

$\varepsilon = 3 \times 10^{-6}$ sec^{-1}
$A = 0.6 \times 10^{-6}$ sec^{-1}
$\lambda^2 = 2.5 \times 10^{-12}$ m^{-2}
$\sigma_B = 1.18 \times 10^{-7}$ cal cm^{-2} day^{-1} deg^{-4}
$\Gamma = 0.95$
$N_1 = 1.30$
$N_2 = 0.81$
$X = 0.26$
$r_a = 0.32$

Whenever we have included the exchange processes between the eddies and the zonal current we have used the following values of the exchange coefficients

$K_1 = 0.8 \times 10^6$ m^2 sec^{-1}
$K_3 = 2.0 \times 10^6$ m^2 sec^{-1}
$K_H = 1.45 \times 10^6$ m^2 sec^{-1}

The small-scale convection is characterized by the empirical constants b and c. Whenever this process has been included in an experiment we have used the values

$b = 8.31$ cal cm^{-2} day^{-1} deg^{-1}

$c = -196.41$ cal cm^{-2} day^{-1}

The evaporation and condensation processes in the model are characterized by the parameters w, e, f. The empirical constants e and f had the values

$e = 1.27$

$f = -80.12$ cal cm^{-2} day^{-1}

The empirical values for the constants b, c, e and f were adopted from Saltzman (1968). The remaining coefficients which have not been assigned a specific value as yet are r_s, w and k. They are the three parameters which in addition to ε, deal specifically with the surface conditions. It is perfectly obvious that it is impossible to assign realistic values to these parameters, mainly because of great differences between the conditions over land and over water, but also because of variability of these coefficients depending on other parameters. We shall again follow Saltzman (1968) and consider a typical land situation, a typical ocean situation and an intermediate case as outlined in Table IV.

Table IV

Values of surface state parameters

Case	k, calcm^{-2} day^{-1} deg^{-1}	w	r_s
a) ocean	100	1.0	0.10
b) intermediate	10	0.9	0.15
c) land	1	0.8	0.20

The experiments which have been carried out can for purposes of presentation be ordered in a series of increasing complexity. We shall name the experiments according to the processes listed in Table I. For example, if an experiment is listed as $n = 1,2$ it means that the heating is determined using only the short-wave solar radiation and the long-wave radiation. If processes $n = 4$ or 5 are included we shall add the notation a, b, c referring to Table IV. The values of K_1, K_3 and K_H are used as listed above in all experiments except the very first in the list below.

List of experiments:

1. $n = 1, 2$ $\qquad K_1 = K_3 = K_H = 0$
2. $n = 1, 2$
3. $n = 1, 2, 5, a$
4. $n = 1, 2, 5, b$
5. $n = 1, 2, 5, c$

6. $n = 1, 2, 3, 5, a$
7. $n = 1, 2, 3, 5, b$
8. $n = 1, 2, 3, 5, c$
9. $n = 1, 2, 3, 4, 5, a$
10. $n = 1, 2, 3, 4, 5, b$
11. $n = 1, 2, 3, 4, 5, c$

For each of these 11 experiments we shall first give the computed values of the maximum and minimum A_z and K_z and the time of occurrence. These values listed in Table V may then be compared with the observed values as listed in Table III.

Table V

Maximum and minimum values of A_z and K_z and the time of occurrence

	A_z		K_z	
Exp. No.	Max	Min	Max	Min
1	15740 30	356 190	1899 20	147 200
2	9311 30	91 180	3828 40	76 200
3	2518 30	814 190	1055 40	380 200
4	3953 30	387 190	1638 40	205 200
5	6799 30	86 190	2800 30	73 200
6	3466 30	1422 190	1451 40	644 200
7	5182 30	533 190	2144 40	274 200
8	7529 30	89 190	3099 30	76 200
9	3319 30	1322 190	1390 40	601 200
10	3972 30	396 190	1646 40	210 200
11	4546 30	83 190	1875 40	69 200

The values listed in Table V show very clearly the improvements in the predicted annual variation as we gradually include more physical processes in the determination of the heating function in the model. Experiment No. 1 is included in order to illustrate the well known fact that a very large temperature gradient will exist between pole and equator if we restrict

the heating to the processes of radiation and consider the axi-symmetrical flow without interaction with the eddies. Experiment No. 2 shows how the temperature gradient between pole and equator is reduced significantly by incorporating the exchange processes between the eddies and the zonal flow. This experiment (No. 2) corresponds to the case considered by Sela and Wiin-Nielsen (1971) as far as the physical processes are concerned, although the method of solution of the model equations is different in the two cases.

Nos. 3, 4 and 5 demonstrate quite clearly the effects of the subsurface conduction in reducing the amounts of available potential energy to a magnitude comparable with the amounts found in the atmosphere. It is seen that $k = 1$ (No. 5) gives results rather close to $k = 0$ (No. 2), but the results of experiments No. 3 and 4 indicate that some intermediate value of k may give the correct amount of A_z, max, although all the results for A_z, min, in this category (Nos. 3, 4 and 5) are too small as compared with observations. Some improvement in this regard is found in the next set of experiments (Nos. 6, 7 and 8) where we have added the effect of small scale convection. It is to be noted that the addition of the convection increases the value for A_z, min, especially for the larger values of k (Nos. 6 and 7). We note finally that the addition of the condensation and evaporation processes in experiments No. 9, 10 and 11 seems to result in relatively small changes in the solution, again for the large values of k which on the whole seem to be the most realistic.

The time of occurrence of the maximum and minimum values of A_z and K_z given in Table V are given as a multiple of 10 simply because the values were printed for every 10 days. It is, however, obvious that the time of maximum and minimum energy is not at all sensitive to the physical processes included in the model. Note, for example, that A_z has a maximum on the 30th day in each of the 11 experiments. Similarly, the maximum of K_z occurs on the 40th day in all cases except experiment No. 5. We may therefore state as a general result that the models behave well in predicting the time of maximum and minimum energy, and that the maximum amount of K_z occurs some days later than the maximum amount of A_z.

Table VI

Annual mean values of energy parameters for the various experiments. Unit: watts m^{-2}

Exp. No.	$G(A_z)$	$C(A_z, A_E)$	$C(A_z, K_z)$	$C(K_E, K_z)$	$D(K_z)$
1	2.48	0.00	2.48	0.00	2.48
2	4.16	4.10	0.06	1.12	1.18
3	1.78	1.72	0.06	0.42	0.48
4	2.22	2.16	0.06	0.55	0.61
5	3.18	3.12	0.06	0.84	0.90
6	2.54	2.46	0.08	0.60	0.68
7	2.88	2.82	0.06	0.74	0.80
8	3.48	3.42	0.06	0.93	0.99
9	2.42	2.34	0.08	0.57	0.65
10	2.24	2.18	0.06	0.56	0.62
11	2.20	2.16	0.04	0.57	0.61
Observations	2.2	2.9	0.3	0.2	0.5

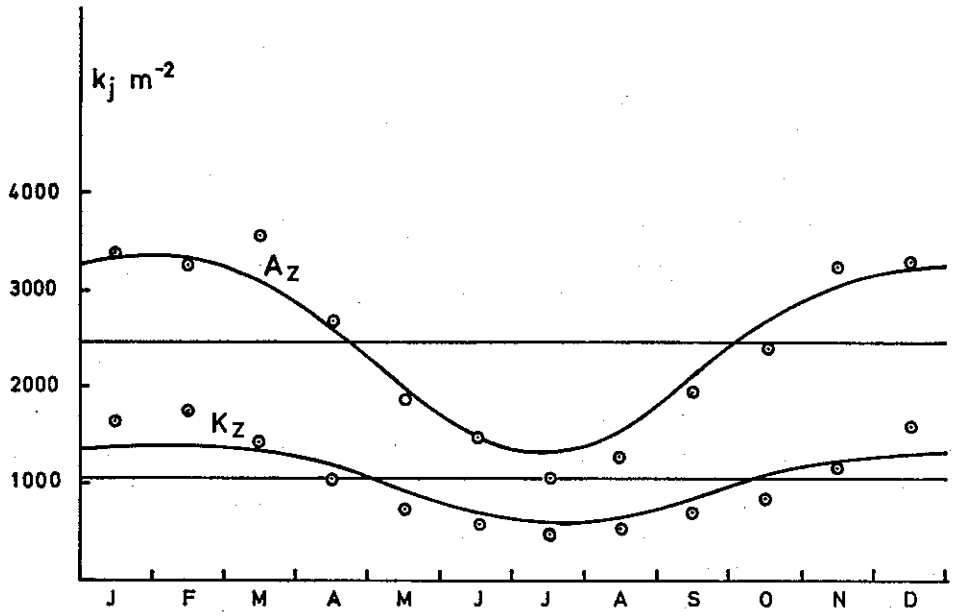

Fig. 1A: The annual variation of zonal available potential energy and zonal kinetic energy in exp. No. 9. Unit: kj m^{-2}. Circles are observed values for the year 1963, adjusted in such a way that they have the same annual average as the theoretical values.

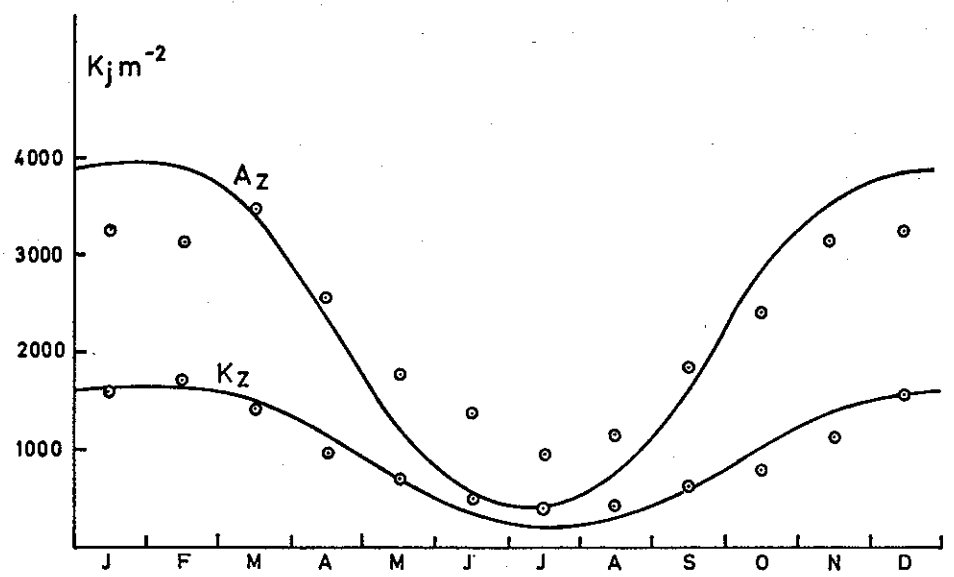

Fig. 1B: As Fig. 1A, but for exp. No. 10.

It is also of interest to consider the generation, conversion and dissipation rates for the experiments. Table VI gives the annual mean values of $G(A_z)$, $C(A_z, A_E)$, $C(A_z, K_z)$, $C(K_E, K_z)$ and $D(K_z)$ for the eleven experiments. It is seen that the numerical values of k are quite important in determining the intensity of the circulation in the first series of experiments (see for example Nos. 3–5 and Nos. 6–8). However, when all processes are included (Nos. 9–11) it turns out that only minor changes are found in the annual mean values. As we shall see later there are still significant differences between Nos. 9, 10 and 11.

Values based upon calculations using a quasi-geostrophic formulation and atmospheric data (Wiin-Nielsen, 1968 b) are entered in the last line of Table VI. It is seen that the last experiments in the series agree reasonably well with the values based upon observations. The main difference is that $C(K_E, K_z)$ is somewhat larger in the experiments than in the observational studies.

Among the experiments listed in Table V and Table VI we have selected the last group (Nos. 9–11) for a detailed analysis. The reason is that this group contains all the processes considered in the calculations. Some of the results of experiment No. 1 are given in the Appendix to this paper, because this experiment considers the solution for the axi-symmetrical circulation under radiational equilibrium. It corresponds therefore within the limitations of this model to the classical speculations on the nature of the general circulation, and the results have at least a pedagogical value.

The annual variations of A_z and K_z are given in Fig. 1A for No. 9 and in Fig. 1B for No. 10. The unit for the amounts of energy is kjm^{-2}. On each of the two figures we have also entered the observed annual variation as obtained from the data for the year 1963. These data are taken from Table 1 in the paper by Wiin-Nielsen (1967), and are shown by circles. The observed data has in each case been adjusted in such a way that they have the same mean value as the computed values. It is seen that the computed annual variation of A_z is essentially correct in No. 9 (Fig. 1A), while the annual variation of A_z as computed in No. 10 (Fig. 1B) is too large. With respect to kinetic energy we find a computed annual variation which is somewhat too small in Fig. 1A and a little too large in Fig. 1B.

Figs. 2A and 2B show the annual variation of $G(A_z)$, $C(A_z, K_z)$ and $D(K_z)$ in the unit: watts m^{-2}. The most important feature in these figures is the lag between $G(A_z)$ and $D(K_z)$, which is comparable to the lag found in studies based upon observations, Wiin-Nielsen (1967). We notice that $G(A_z)$ in general is much larger than $D(K_z)$, which in turn is larger than $C(A_z, K_z)$. These features are in agreement with observational studies. Figs. 2A and 2B show that the larger annual variation found in Fig. 1B as compared with Fig. 1A is accompanied by a similar larger annual variation in Fig. 2B as compared with Fig. 2A. In Figs. 3A and 3B we have shown the annual variation of $C(A_z, A_E)$ and $C(K_E, K_z)$ as computed in experiments No. 9 and 10, respectively. We notice that $C(K_E, K_z) < C(A_z, A_E)$ throughout the year, and that both of the energy conversions remain positive in agreement with the average behaviour of the atmosphere.

Fig. 4 shows the annual variation of the total potential energy, defined as the sum of the internal and potential energies. It is well known that $P + I$ can be computed from the formula

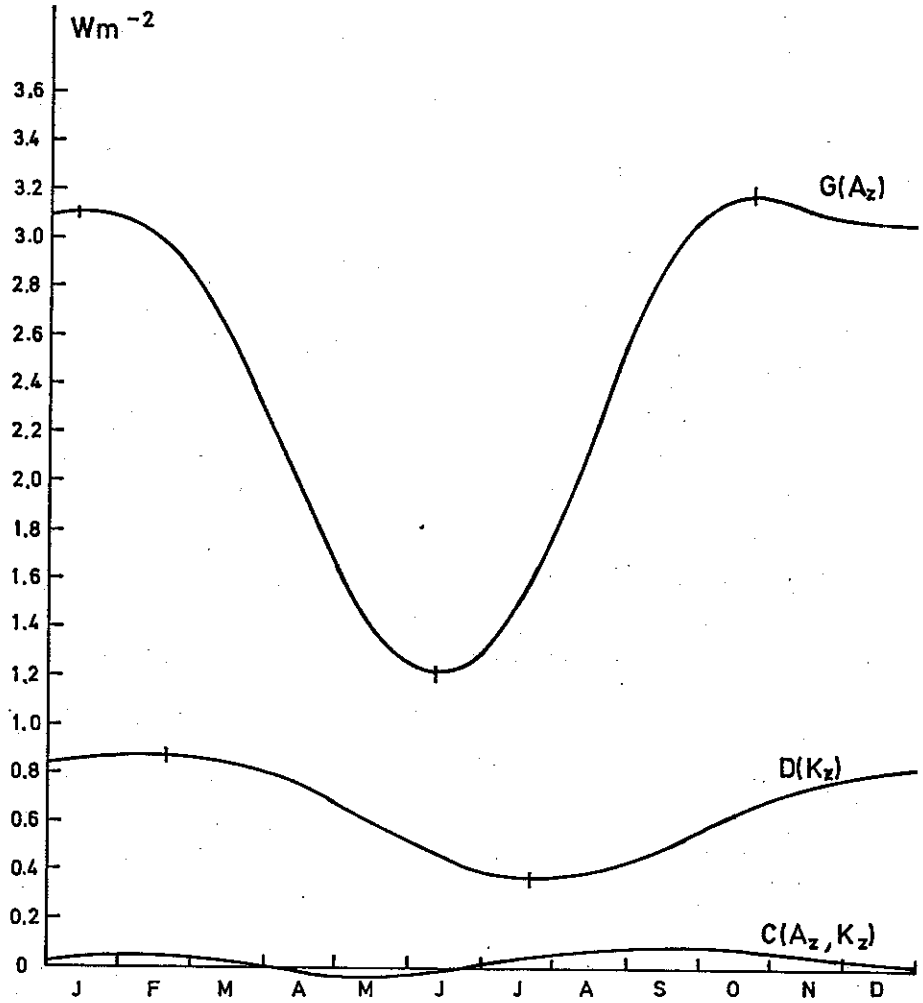

Fig. 2A: The annual variation of the generation of zonal available potential energy, the conversion of this form of energy to zonal kinetic energy, and the dissipation of zonal kinetic energy in exp. No. 9. Unit: watts m^{-2}

$$P + I = \frac{1}{2\pi a^2} \frac{1}{g} \int_0^{p_0} \int_0^{\pi/2} \int_0^{2\pi} C_p T a^2 \cos\varphi d\lambda d\varphi dp \tag{3.1}$$

In our simple two level model we have only one temperature in each vertical column. It is then seen from (3.1) that $P + I$ becomes proportional to the area mean temperature. We notice that $P + I$ has a maximum in August and a minimum in early February in experiment No. 9, while the corresponding times in No. 10 are middle January and mid-July. In each case we find a lag between the minimum and maximum mean temperature and the winter and summer solstices. These features are in agreement with a recent observational study by Oort (1971).

Based upon the information in Figs. 1–4 we may conclude that the model calculations reproduce the essential parts of the observed energy cycle in the zonally averaged quantities in the atmosphere. There are no differences between the computed and the observed energy

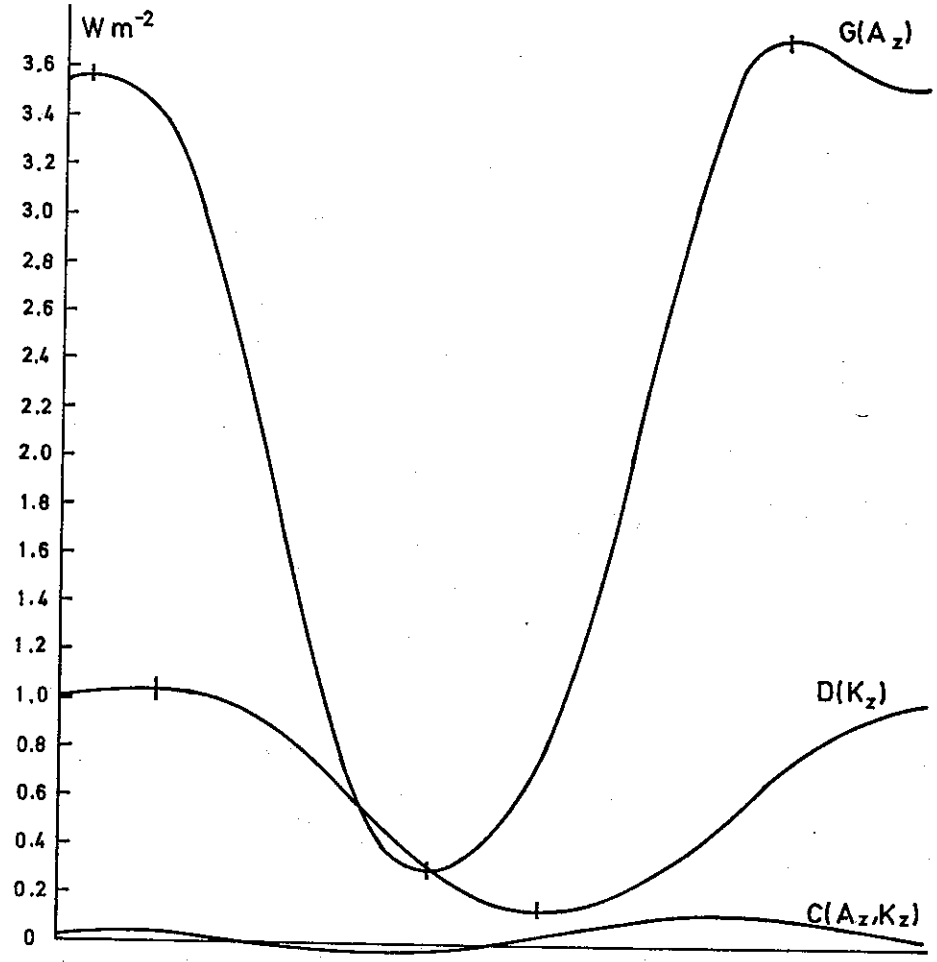

Fig. 2B: As Fig. 2A, but for exp. No. 10.

generations, conversions and dissipations with respect to the direction of the energy flow. The theoretical calculation is also capable of reproducing the observed annual variation of A_z, K_z, $G(A_z)$ and $D(K_z)$ with a good degree of accuracy, considering the simplicity of the model.

The original purpose of formulating the present model of the zonally averaged circulation was to simulate the annual variation of the energetics of the atmosphere. As demonstrated above, the experiments have been successful in this regard. However, it is quite possible to have an atmospheric model which describes the energetics correctly, but is still inaccurate in details. It is therefore of some interest to investigate the annual variation of several other parameters entering into the model.

Fig. 5A shows three curves giving the temperature as a function of latitudes for the winter half (January-March, October-December, incl.) the annual mean and the summer half (April-September, incl.) as computed in experiment No. 9. Observed values for the same averaging periods obtained from Peixoto (1960) are also entered on Fig. 5A. It is seen that the computed temperature profiles are in good agreement with the observational studies. However, there

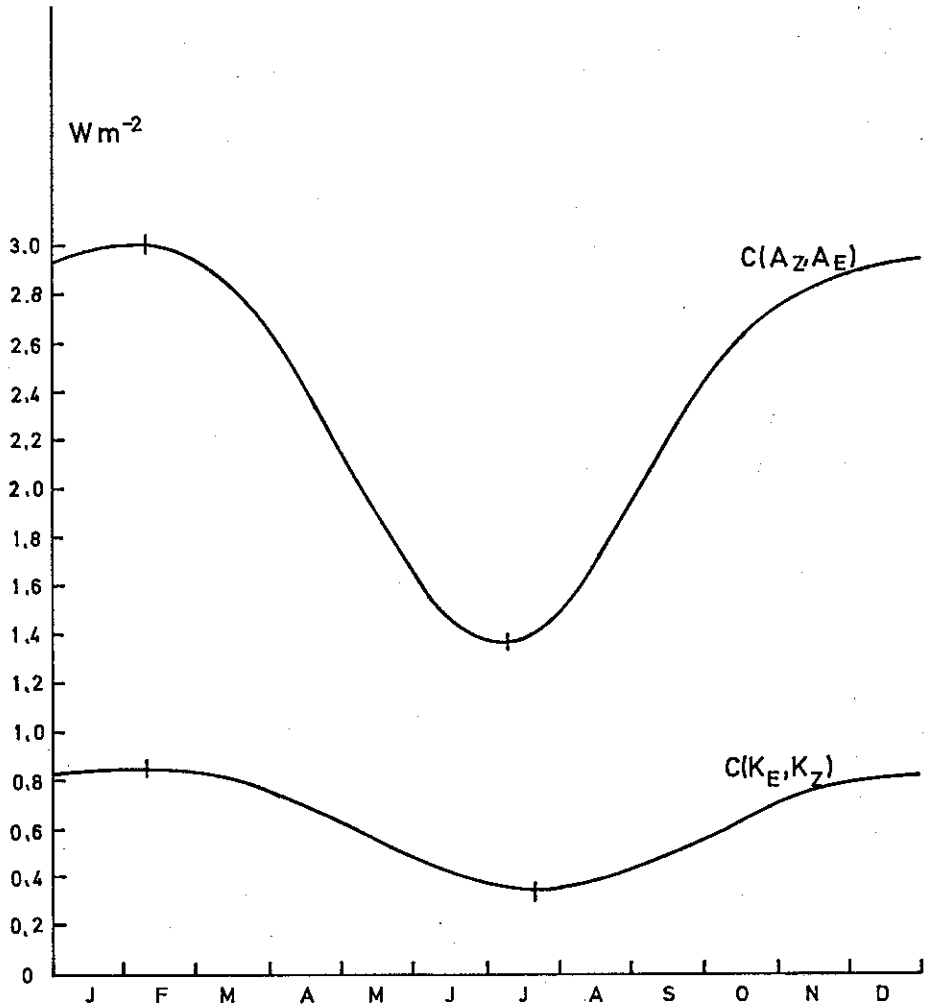

Fig. 3A: The annual variation of the conversion from zonal to eddy available potential energy and the conversion from eddy to zonal kinetic energy. Unit: watts m^{-2}. Exp. No. 9.

are naturally differences. The computed winter temperatures are a little larger than the observed values in middle latitudes, while the computed summer temperatures are a little smaller than the corresponding observed values. We note also that the details of the temperature profile in low latitudes cannot be reproduced with our model in which we have assumed symmetry around the equator.

Fig. 5B corresponds to Fig. 5A, but applies to experiment No. 10. The observed values entered on Fig. 5B are the same as those on Fig. 5A. We notice a somewhat better agreement between the calculations and the observations in Fig. 5B. This is especially true in the high latitudes.

Fig. 6 shows as solid curves the computed temperatures for January and July in exp. No. 10, while the dashed curves are the vertically averaged temperatures based on observations as obtained from Palmen and Newton (1970) as representative for the two months. We observe that the computed temperatures for July are in excellent agreement with the observed values

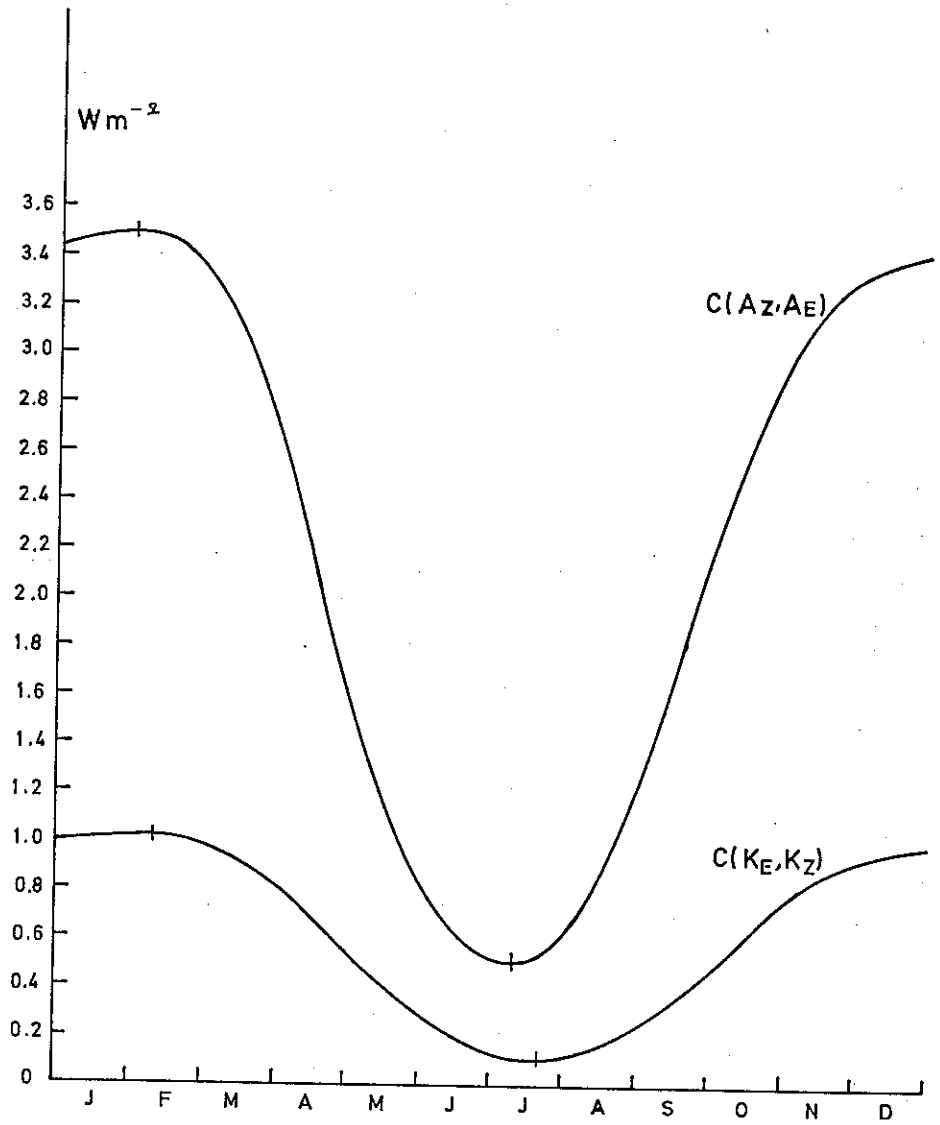

Fig. 3B: As Fig. 3A, but for exp. No. 10.

while the computed January profile has too large values of the temperature, expecially in the high latitudes.

We consider next the annual variation of the zonal wind at the upper and lower levels in the model. Fig. 7 shows the annual variation of the zonal wind at the upper level for exp. No. 10 while Fig. 8 gives the corresponding information for the lower level of the same experiment. The maximum winds at the upper level occur in February at 60°N and are slightly more than 20 m sec^{-1}. There are easterly winds at the very high and the very low latitudes, but the easterlies do not cover as large an area during the summer as is indicated by observations. The position of the maximum zonal wind at the upper levels is much further north in the theoretical calculations than is found in observational studies of data from the northern

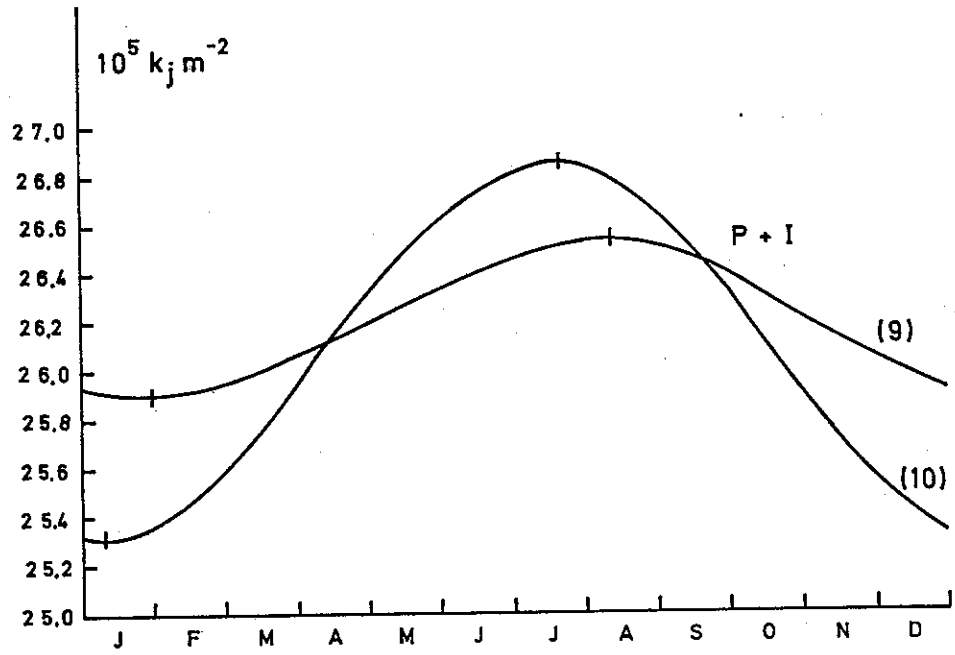

Fig. 4: The annual variation of the total potential energy in exp. No. 9 and exp. No. 10. Unit: 10^5 kj m^{-2}.

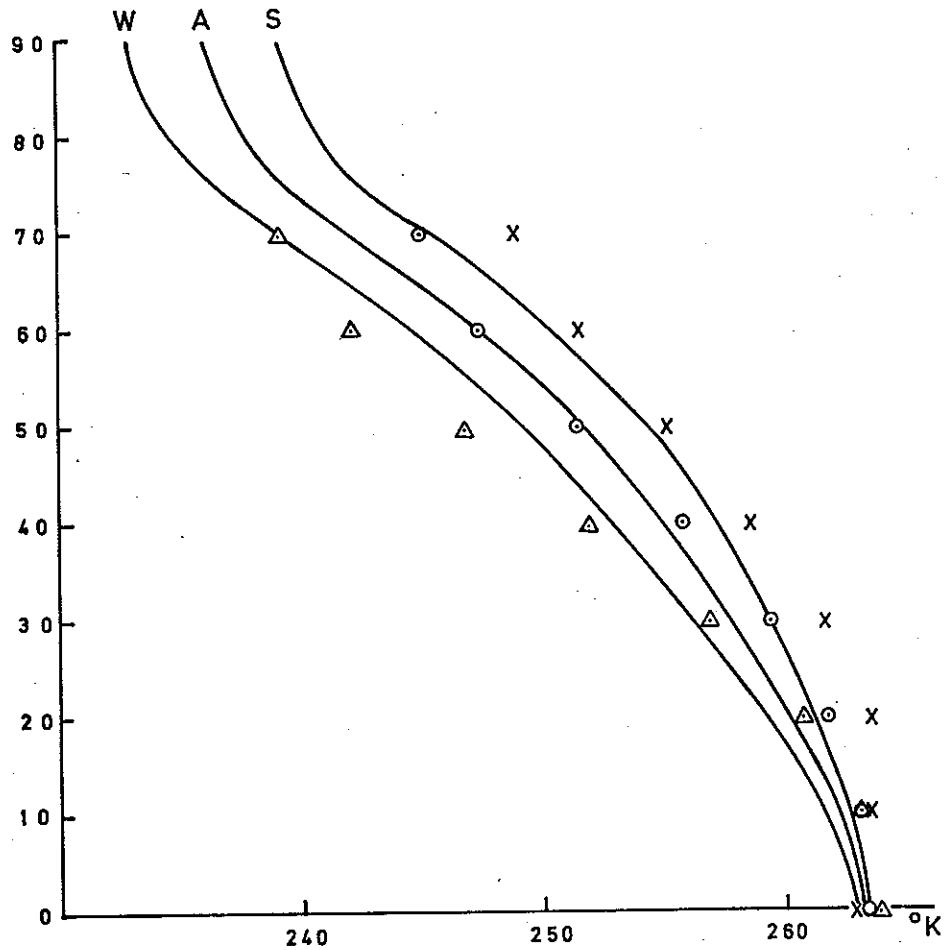

Fig. 5A: The 50 cb temperature as a function of latitude for the winter season (October-March, incl.), the summer season (April-September, incl.), and the annual average as computed in exp. No. 9. Observed values from Peixoto (1960) are also entered (triangles for winter, crosses for summer, and circles for the annual average).

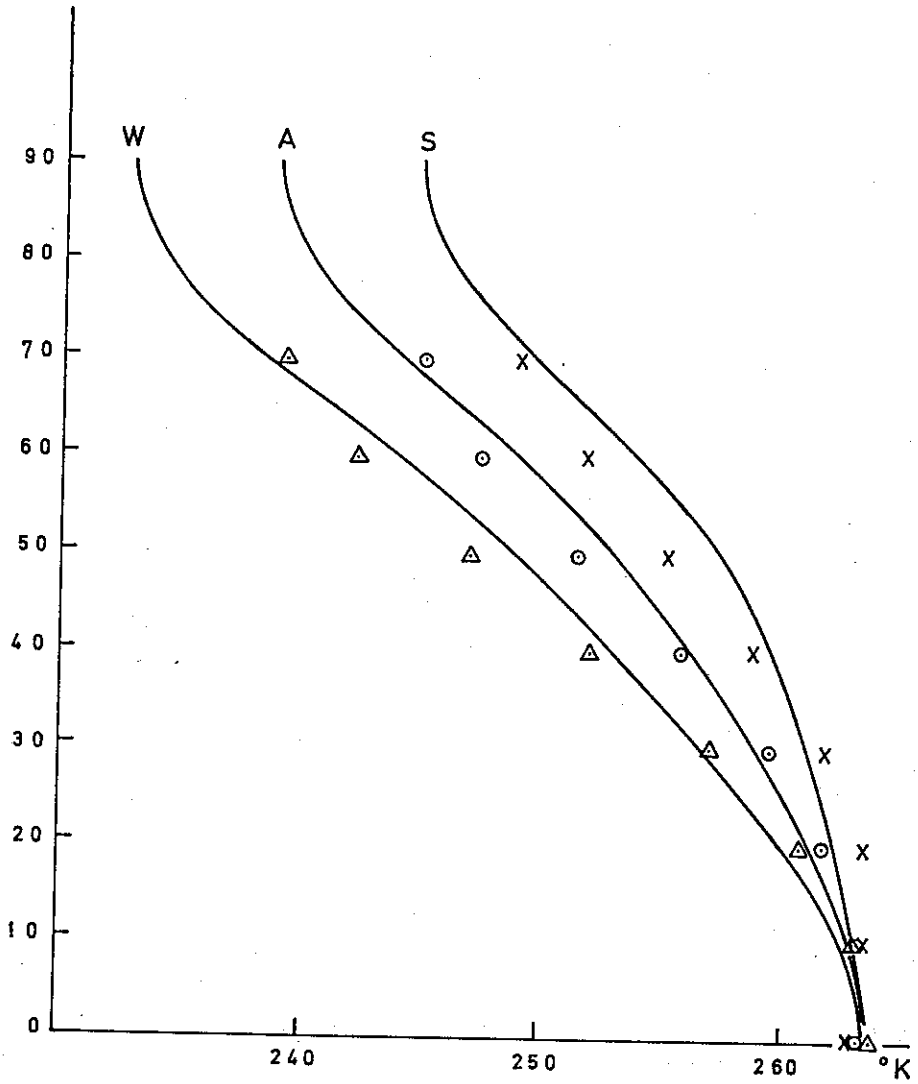

Fig. 5B: As Fig. 5A, but for exp. No. 10.

atmosphere. The distribution with respect to latitude is in somewhat better agreement with observational studies using data from the southern hemisphere, where there is a tendency for a rather broad maximum during winter with rather large wind velocities at high latitudes (Obasi, 1963) (Heastic and Stephenson (1960)). Similar results have also been obtained by Jenne et al. (1968). The annual variation of the zonal wind at the lower level (Fig. 8) is in much better agreement with observational studies (Buch, 1954, Crutcher, 1959, 1961). The discrepancies between the distributions in Figs. 7 and 8 and observed distributions can be traced to the errors in the predicted temperatures. Note on Figs. 5A and 5B that the calculated temperature gradient is larger than the observed temperature gradient in the region 60–80°N while the reverse is true in the region 20–40°N. Consistent with these errors we have a thermal wind which is too large in the region 60–80°N and too small in the interval 20–40°N, resulting in zonal winds which are too large in the first and too small in the second region. These errors

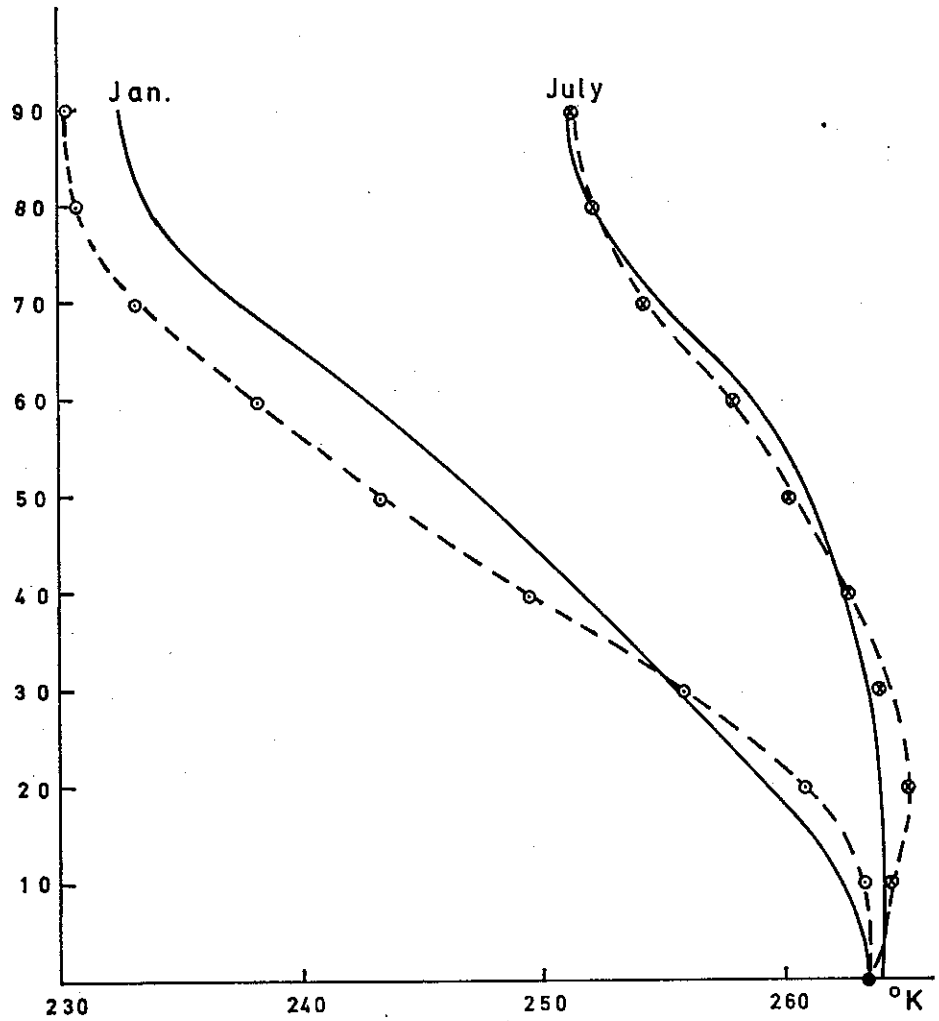

Fig. 6: The computed 50 cb temperatures as a function of latitudes for January and July for exp. No. 10 (solid curves). The dashed curves (circles for January, crosses for July) are vertically averaged temperatures based on observations for the two months.

in the latitudinal temperature profiles are in turn connected with the rather simple parameterization of the various heating processes (see Table I), in particular the treatment of evaporation and condensation and the latent heat release, and with the quasi-geostrophic nature of the model.

It is well known from numerous observational studies that the eddy kinetic energy is converted into zonal kinetic energy on the average through the year. The present model simulates this condition realistically as can be seen from Figs. 3A and 3B. In order to maintain this condition it is necessary that the convergence of the horizontal momentum transport by the eddies is positively correlated with the zonal wind. Figs. 9 and 10 show the transport of angular momentum at the upper and lower levels, respectively, as a function of latitude and time. It is seen that the transport of angular momentum by the eddies in the model agrees in a qualitative sense with the results of observational studies as summarized by Lorenz (1967). We note that the angular momentum transport is of the same order of magnitude as the

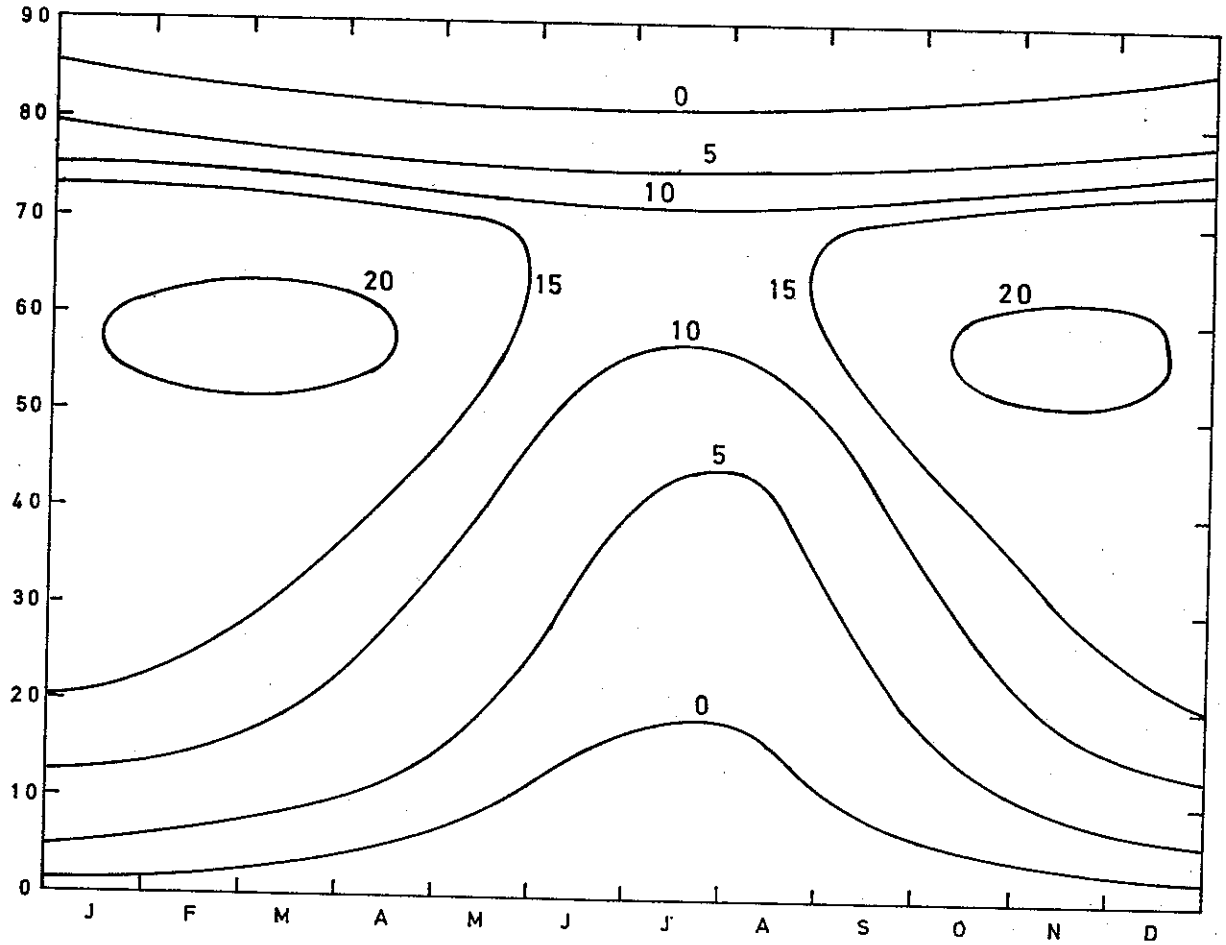

Fig. 7: The zonally averaged wind at the upper level (25 cb) as a function of latitude and time. Unit: msec^{-1}. Exp. No. 10.

observed transport, that the distribution with respect to latitude at each level is such that a northward transport is calculated in the low and middle latitudes, while a southward transport is calculated in the high latitudes. In agreement with observations we find also a larger magnitude of the angular momentum transport at the upper level than at the lower level.

Fig. 11 shows the annual average of the angular momentum transport at the two levels as a function of latitude. It is apparent from this figure as well as from Figs. 9 and 10 that the relative magnitude of the angular momentum at the two levels differs from the values obtained from observations. The same remark applies for the relative magnitude of the positive and the negative transports in the low and the high latitudes. Fig. 12 shows the annual average of the total angular momentum transport across the latitude circles through the total depth of the atmosphere.

We consider next the meridional transport of sensible heat by the eddies. This transport can be evaluated at the 50 cb level in the model. Fig. 13 shows the eddy heat transport as a function of latitude and time in the unit: 10^{14} watts/10 cb. This unit is selected in order to ease the comparisons with the diagrams presented by Lorenz (1967) based on the study by

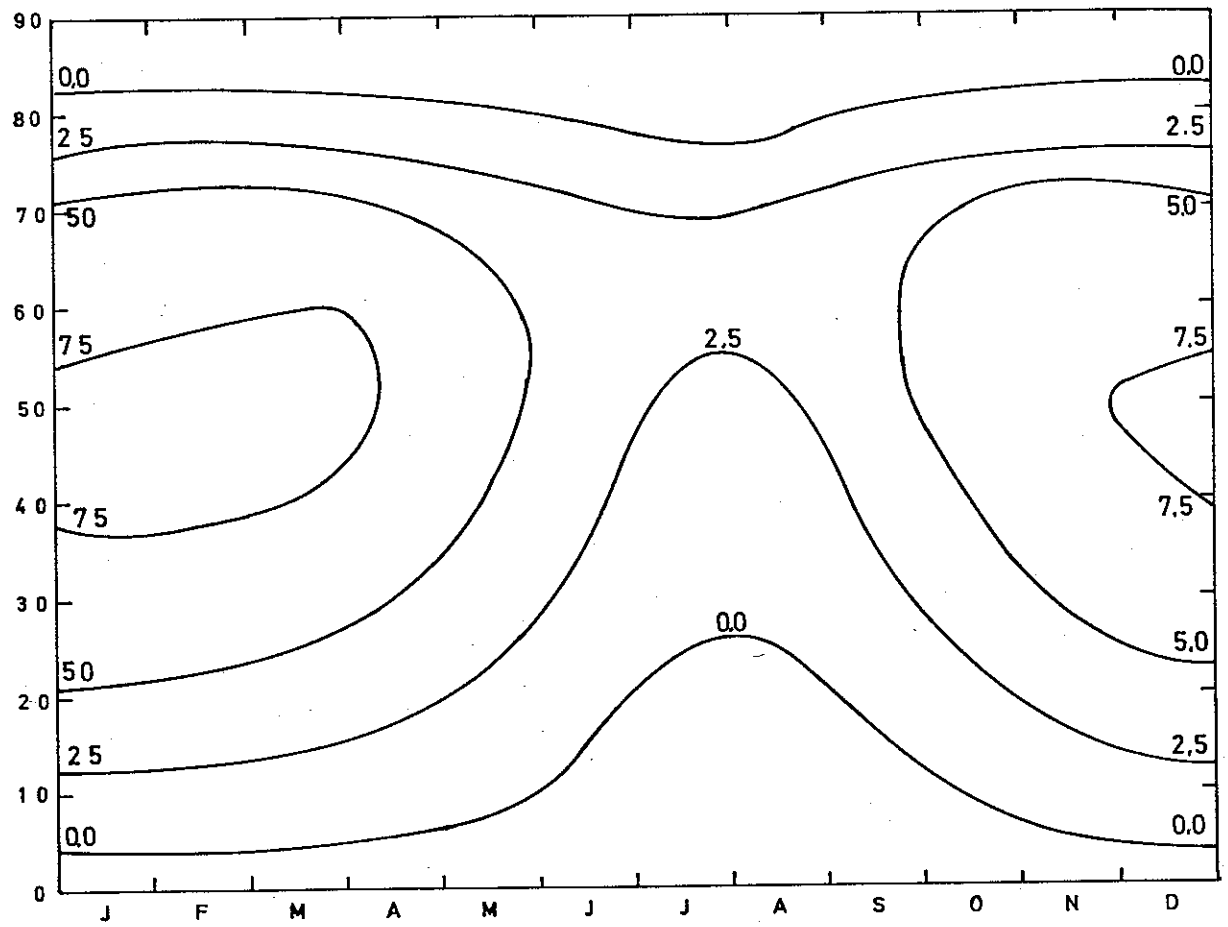

Fig. 8: The zonally averaged wind at the lower level (75 cb) as a function of latitude and time. Unit: $msec^{-1}$. Exp. No. 10.

Peixoto (1960). It is seen that the computed eddy heat transport is of the correct order of magnitude, and that a single maximum is found in middle latitudes, and that the position of the maximum moves from a position at 35°N in winter to 60°N in summer. We notice that the computed eddy heat transport does not show the negative values in the low latitudes found in Peixoto's study (loc. cit.). This feature is related to the fact that we do not reproduce the reverse temperature gradient in the very low latitudes as mentioned in connection with the discussion of Figs. 5 and 6.

Fig. 14 shows the average northward transport of sensible heat by the eddies for the year in the unit 10^{14} watts. The computed transport shows a rather broad maximum located at 50°N in agreement with observational studies. The maximum value in the theoretical calculation is somewhat smaller than the maximum value formed by Peixoto (1960).

Just as it has been possible to evaluate the momentum transport and the heat transport from the parameters predicted by the model by using the parameterization of the transport processes, it is equally possible to determine the heat sources, as a function of latitude and time from the results of the integration. The required information is in (2.15) and (2.16).

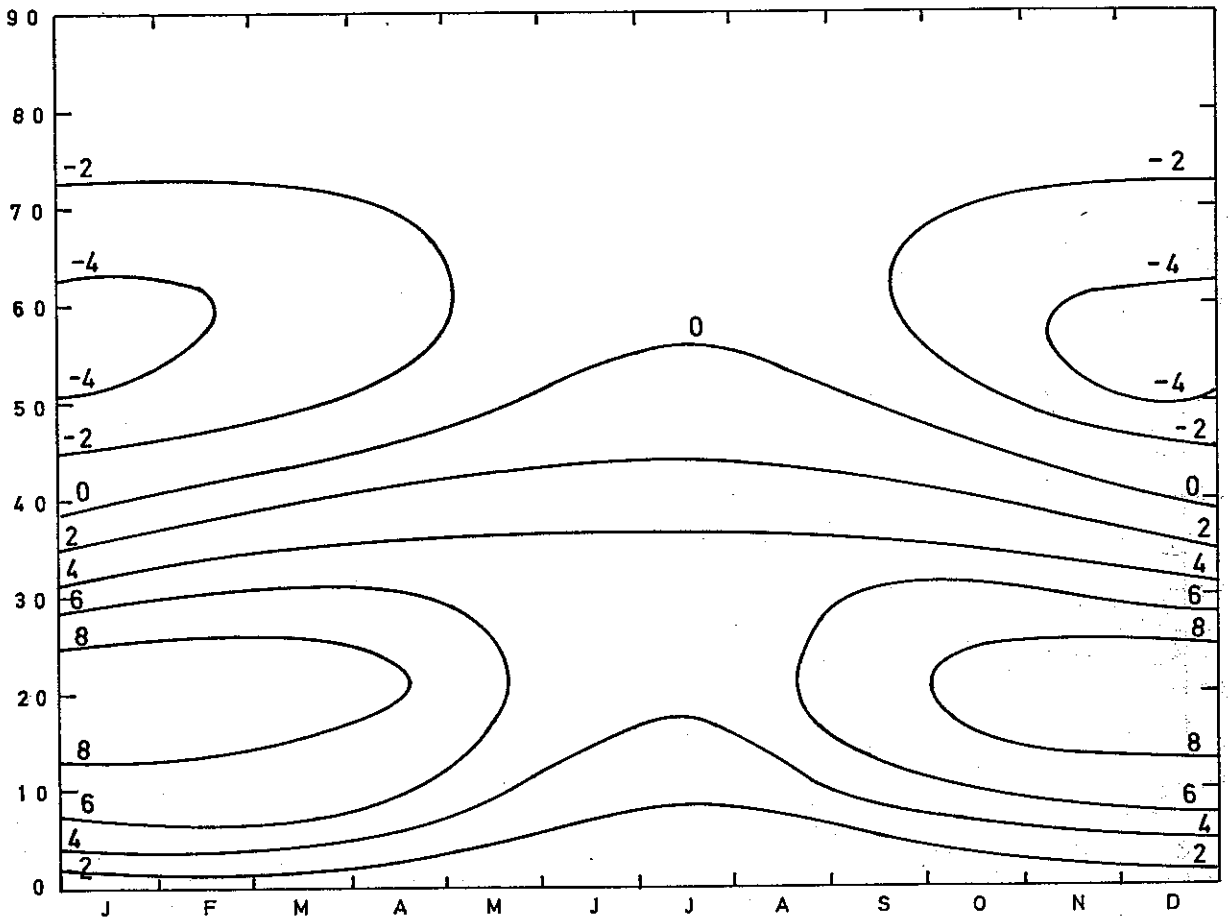

Fig. 9: Angular momentum transport as a function of latitude and time at the upper level (25 cb). Unit: 10^{25}gcm^2 sec^{-2} /10 cb. Exp. No. 10.

Fig. 15 shows the heating as a function of latitude and time in the unit 10^{-2} kj t^{-1} sec^{-1}. Lorenz (1967) gives the annual average of the net gain of energy as derived by Sellers (1966) in the unit: watts m^{-2}. The values given in Fig. 15 may be converted to watts m^{-2} using a conversion factor of 10^2. The major cooling in the atmosphere takes place north of 50°N in the winter and north of 60°N in the summer. South of this region of cooling there is in general a region of warming which occurs around 35–45°N, especially during summer. However, during most of the year there is a weak region of cooling in the region 20–30°N in the results of the model studies, while heating occurs in the equatorial region during the complete year. The magnitudes of the heating and cooling in the theoretical calculation are in general somewhat smaller than those presented by Sellers (1966). In order to ease a comparison we have prepared Fig. 16 which gives the average heating for the winter season and the summer season separately. The computed values of the net cooling in the high latitudes are smaller than Sellers (1966) values by a factor of 2. Similar remarks may be made for the region of heating in the middle latitudes, while the heating at the equator is of approximately the correct magnitude. The region of cooling found in the theoretical calculation around 30°N is not found in the curve

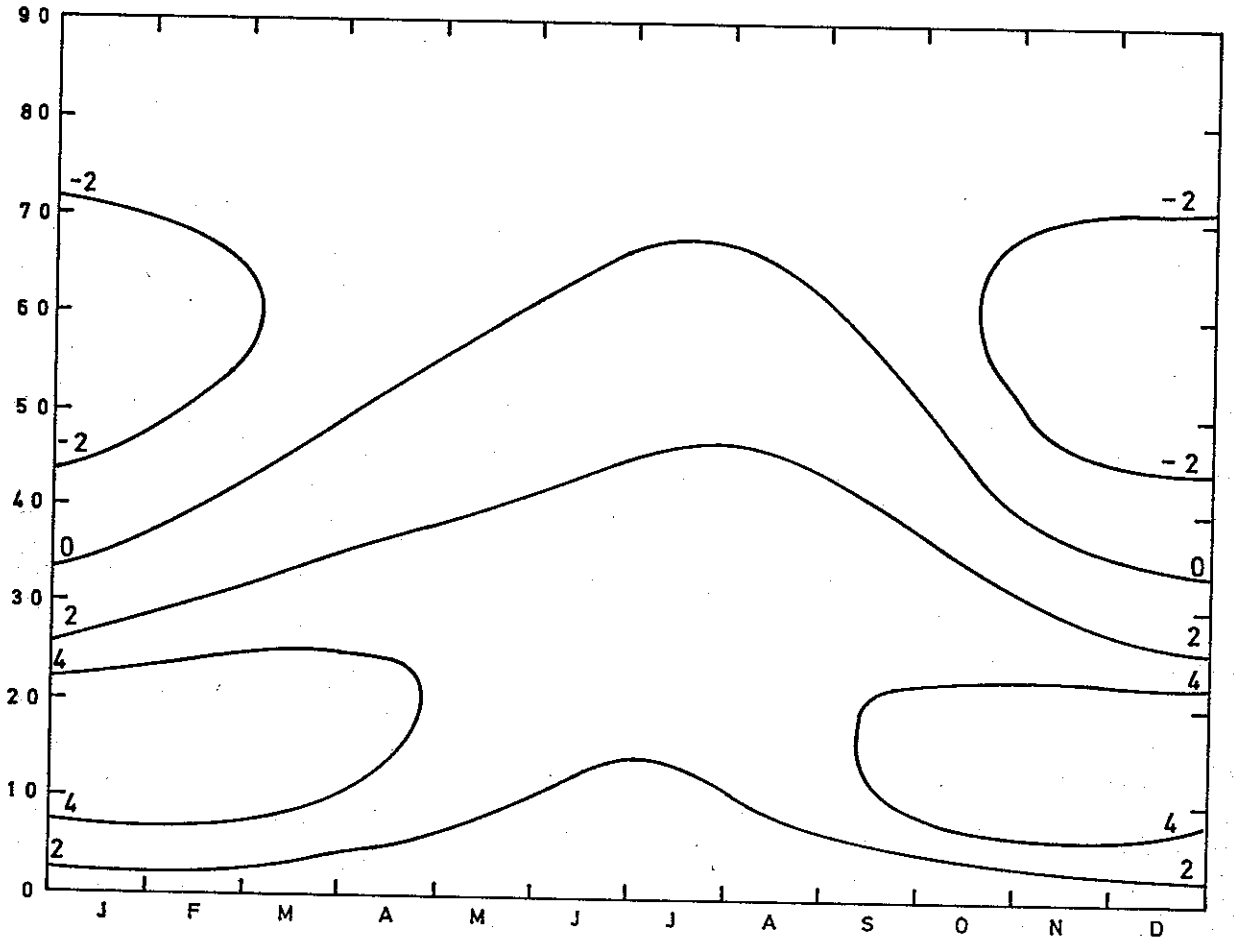

Fig. 10: As Fig. 9, but for the lower level (75 cb).

given by Sellers (1966). However, the tables of the net heating during winter and summer given by Palmen and Newton (1970) indicates that such a region may be found in the atmosphere. The heating calculated in the experiment is also smaller than the values given by Palmén and Newton (1970). The reason for this is to a large extent the quasi-geostrophic nature of the theoretical model and the truncation in the meridional direction in the theoretical calculations.

Knowing the heat sources as described in the previous paragraph and the meridional transport of sensible heat by the eddies as given in Fig. 13, it is possible to calculate the zonally averaged vertical velocity from the thermodynamic energy equation. The local change of the zonally averaged temperature is obtained from the solution of the model equations. Fig. 17 shows the zonally averaged vertical velocity as a function af latitude and time in the unit: mm sec^{-1}. It is seen that the heat sources combined with the effects of the eddy transport result in the well-known three cell mean meridional circulation containing an equatorial Hadley cell, a middle latitude Ferrel cell, and a direct polar cell. The computed values of W_z are of the correct order of magnitude for a quasi-geostrophic model as seen from the

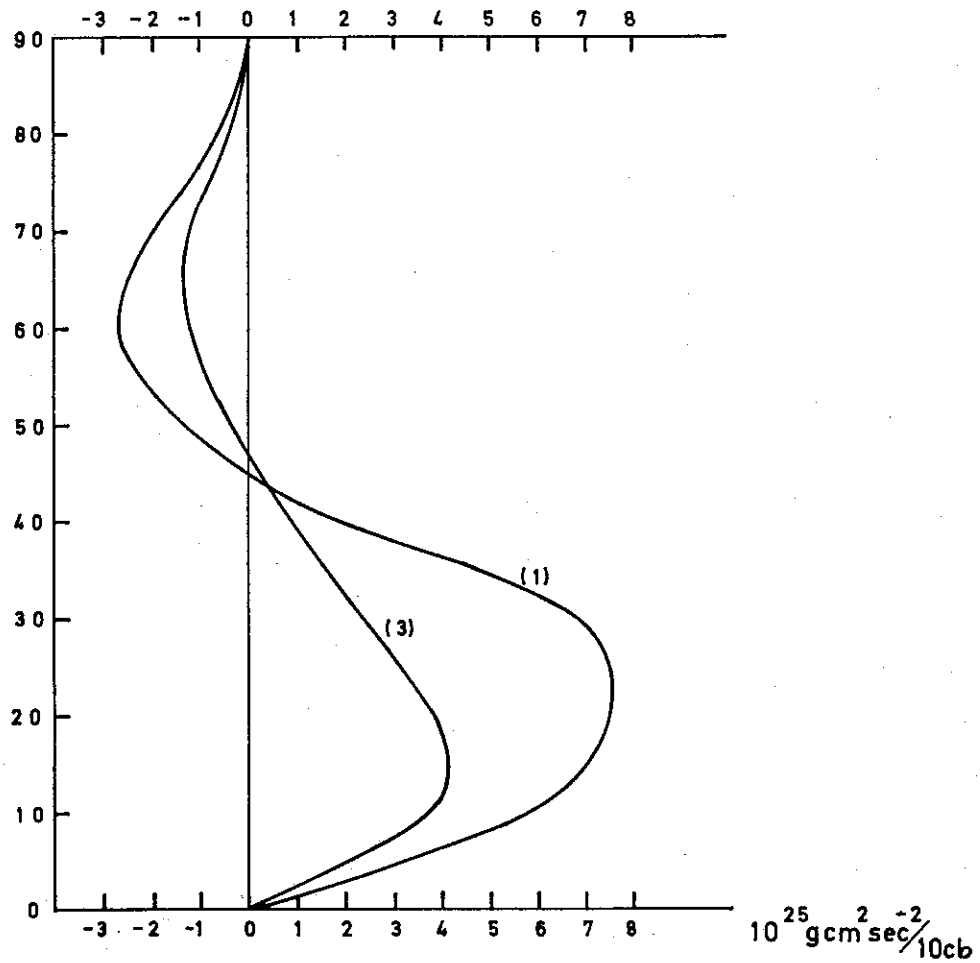

Fig. 11: Annual average of the transport of angular momentum at the upper (1) and the lower level. Unit: 10^{25}gcm^{2}sec^{-2} /10 cb.

observational results by Wiin-Nielsen (1959) and Saltzman and Fleister (1961). However, it is also seen from Figs. 17 and 18, giving the annual mean values of W_z as a function of latitude, that the intensity of the equatorial Hadley cell is less than normally estimated from observations. The reason for this is again the quasi-geostrophic nature of the model and the truncation in the meridional direction.

It is of interest to calculate the temperature in the surface layer of the underlying medium. This can be done from (2.16) using the expressions in Table I, since R_0 and T_D are specified while T_2 is predicted by the model. The computed temperature T_s is then the surface temperature necessary to satisfy (2.16), i.e. to generate no net heat flux across the interface between the atmosphere and the underlying medium. T_s was calculated together with the other diagnostic quantities. Fig. 19 shows T_s in the average for the winter season as computed by the model (exp. 10). The averaged T_D for the same time period is also entered on the figure. It is seen from Fig. 19 that $T_D < T_s$ at all latitudes during winter. This means according to the expression for the subsurface conduction that there is a considerable heat flux upward

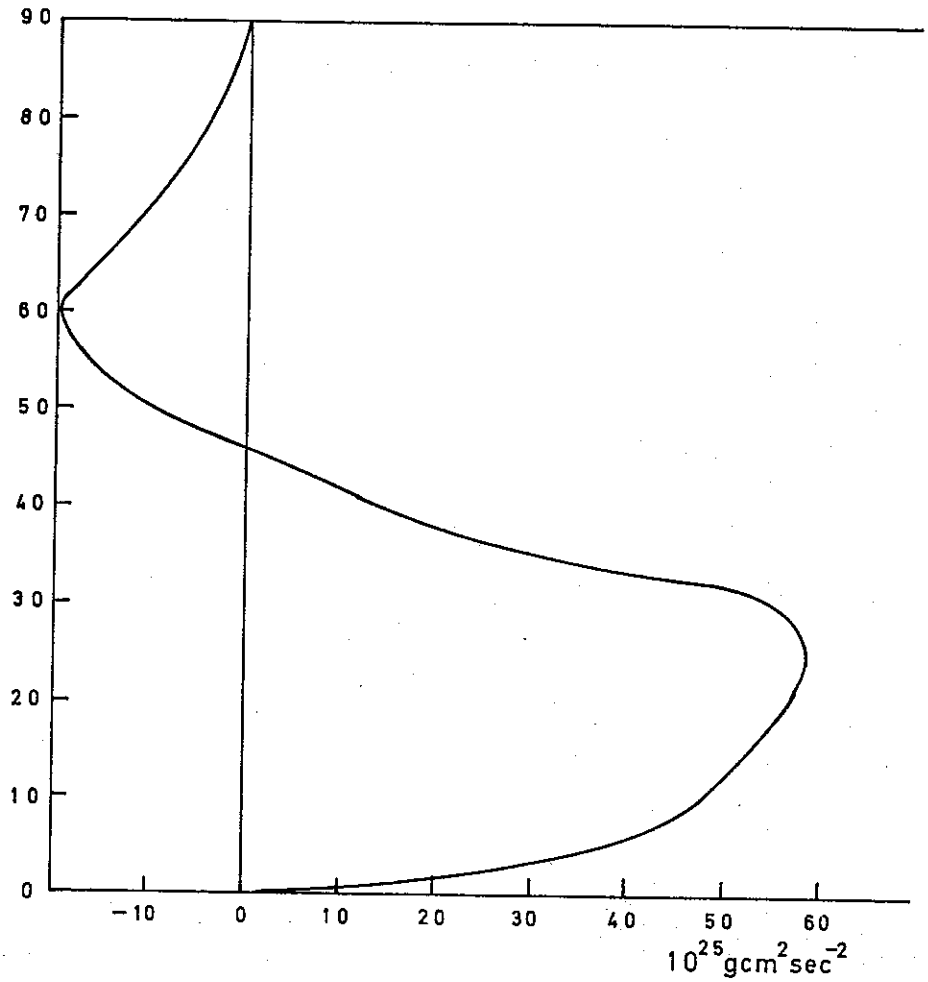

Fig. 12: Annual average of the total transport of angular momentum. Unit: 10^{25}g cm^2 sec^{-2}.

through the underlying medium during the winter season. It is this feature more than any other physical factor which helps to reduce the amplitude of the annual variations as can be seen from Table V. Fig. 20 applies for the summer season, but is otherwise analogous to Fig. 19. We notice that the difference $(T_D - T_s)$ is much smaller in the summer season than in winter, and that there exists a region, from about 40°N to 70°N where $T_D < T_s$, and where the conduction therefore goes away from the surface of the underlying medium.

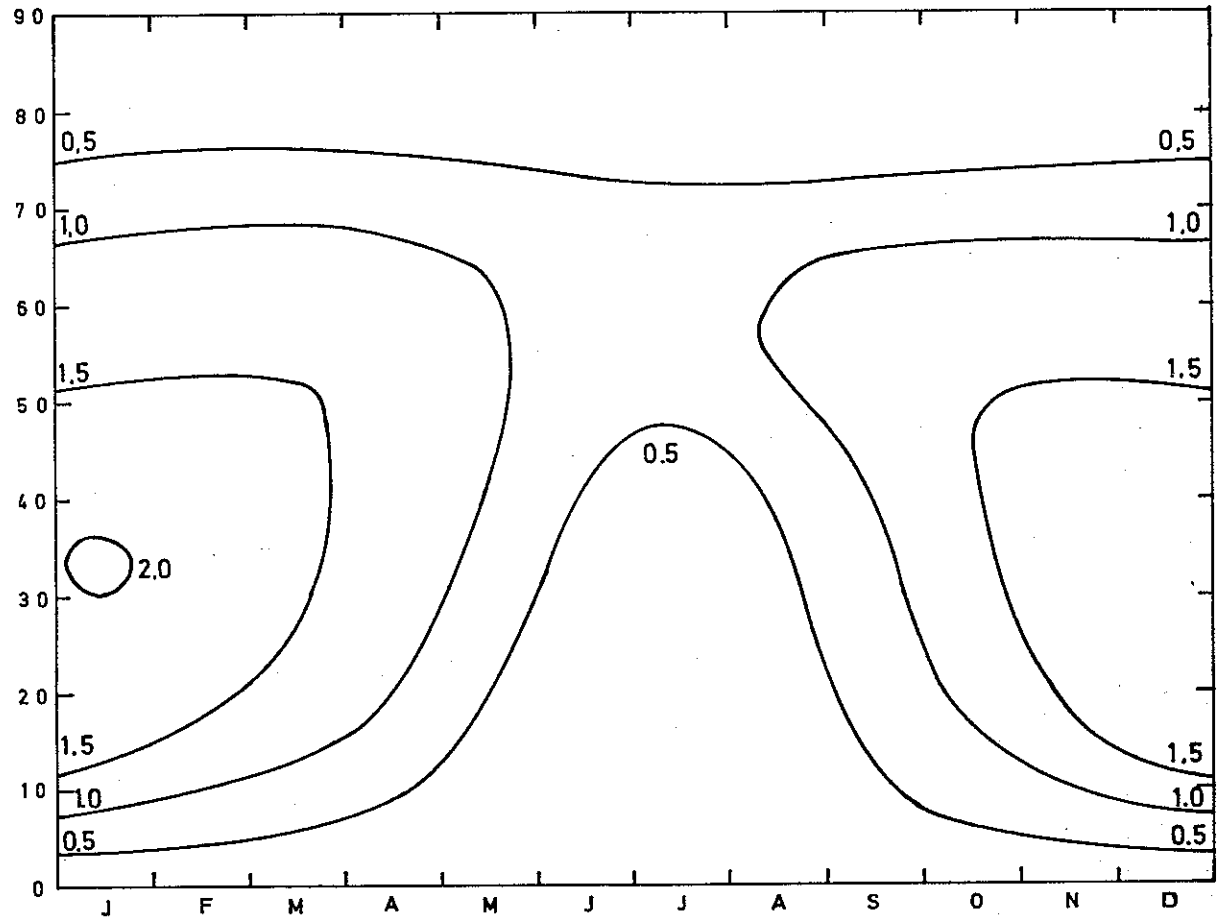

Fig. 13: The transport of sensible heat by the eddies as a function of latitude and time for experiment No. 10. Unit: 10^{14} watts/10 cb.

4. Conclusions. The main purpose of the present investigation was to see if a more detailed description of the heat sources in the meridional plane combined with the parameterization of the exchange processes between the eddies and the zonal average would improve on the theoretical description of the annual variation of the zonally averaged state. It turns out that a much improved description is accomplished by including the various processes outlined in Table I of this paper. While the subsurface conduction and the small-scale convection are reasonably well described in the model, it has only been possible to include the latent heat release in a crude fashion.

The thermal forcing of the model atmosphere is created by specifying the intensity of the solar radiation at the top of the atmosphere and the subsurface temperature as a function of latitude and time of the year. All the physical parameters (albedo, opacity, etc.) listed in the specification of the heat sources and the parameters specifying the exchange processes are assumed to be constant in space and time. These simplifying assumptions are not justified in all cases, and it is to be expected that the solutions obtained to the model equations will contain some distortions due to the assumptions. In spite of the simplicity of the model we

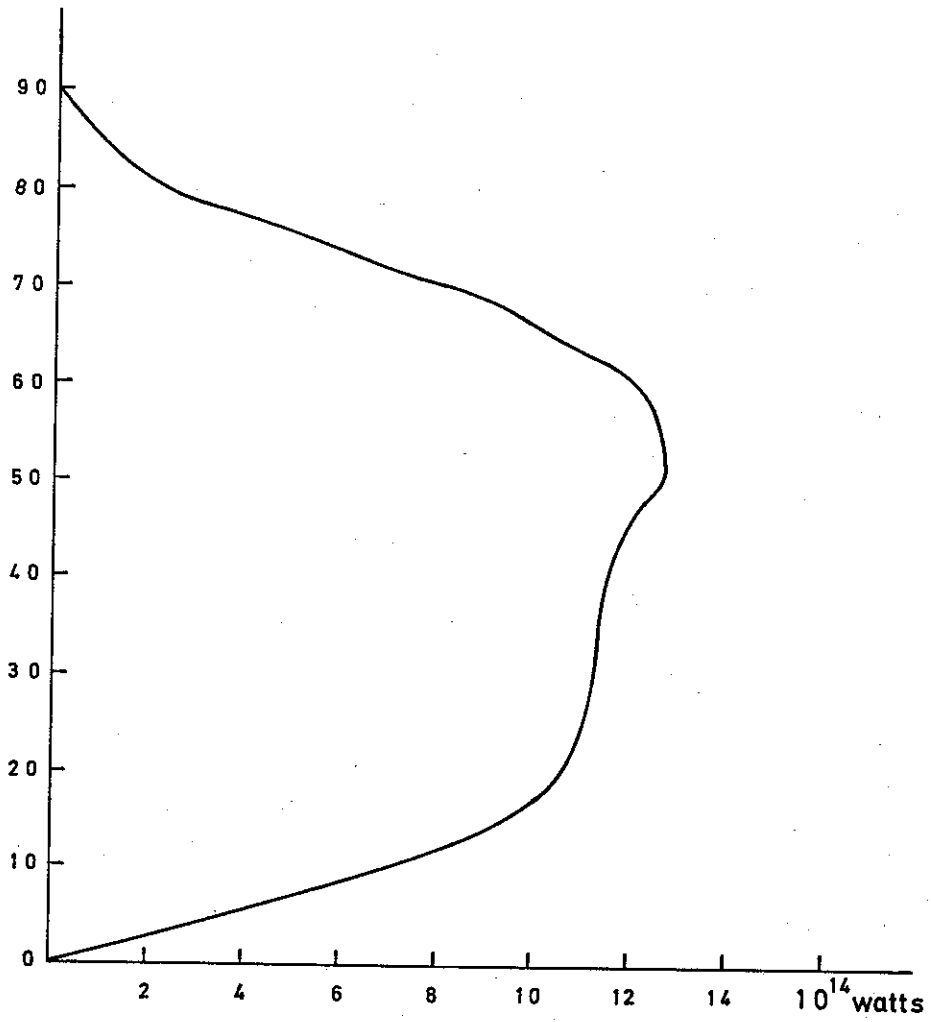

Fig. 14: Annual average of the transport of sensible heat by eddies as a function of latitude for exp. No. 10. Unit: 10^{14} Watts.

obtain in the most complete case included in the experiments a qualitatively correct picture of the annual variation of the zonally averaged general circulation. The amounts of energy, the generations, conversions and dissipations are predicted correctly, and the implied meridional transports of sensible heat and angular momentum show that the parameterization of these transport processes is correct as a first approximation. However, in all the quantities which can be computed from the basic solution of the model equations there is considerable room for improvement. It is possible that some improvement in the results can be obtained by incorporating realistic space and time variations of the physical and empirical parameters. Such experiments should be made in the future. Other improvements, such as a more realistic description of the circulation in low latitudes, can be obtained only be replacing the present quasi-geostrophic model with a more advanced model.

It should finally be pointed out that models of the kind used in this study have their major weakness in the necessary parameterization of the interaction between the eddies and the

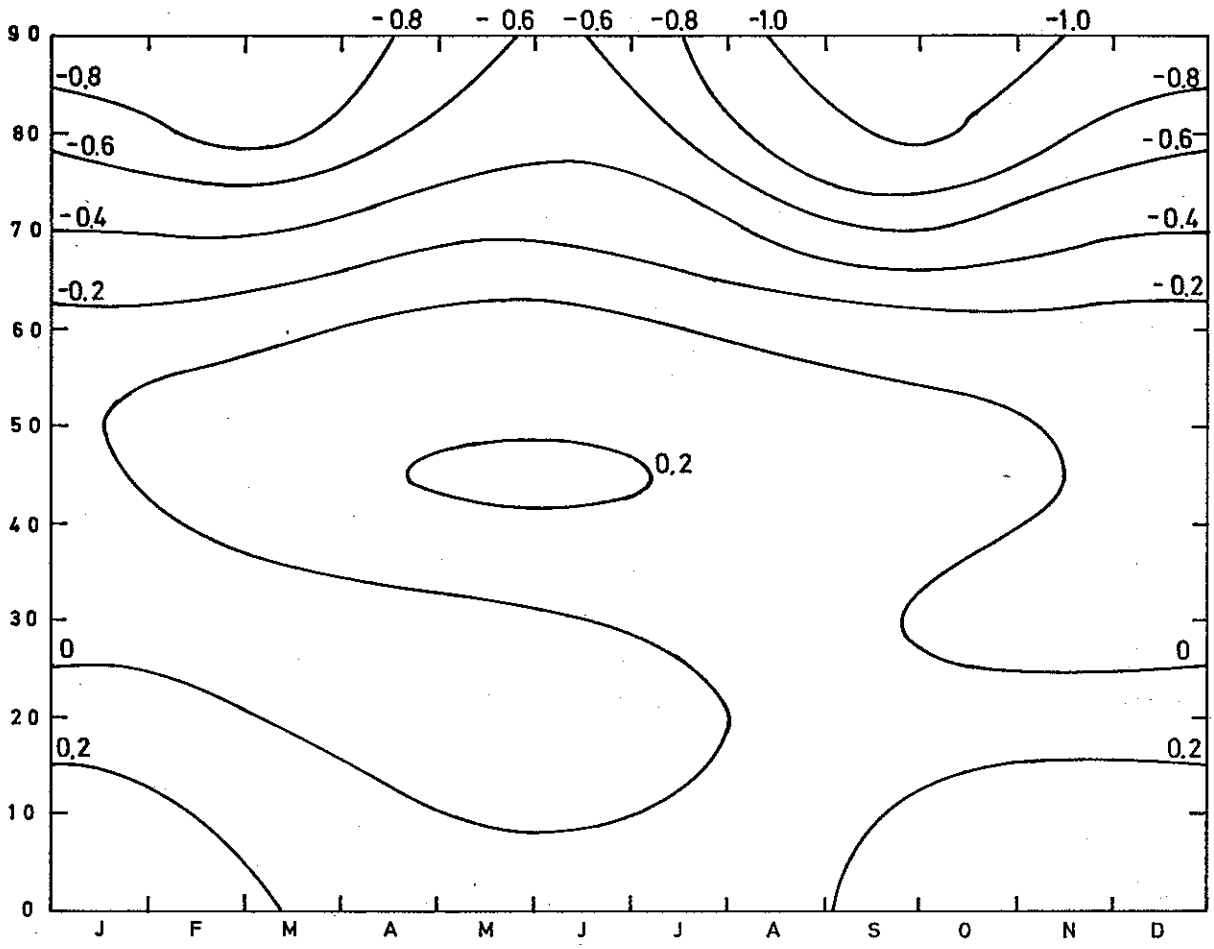

Fig. 15: The heating of an atmospheric column as a function of latitude and time for exp. No. 10. Unit: 10^{-2} kj t^{-1} sec^{-1}.

zonally averaged parameters. While it is possible, at least in principle, to parameterize the interaction for the free, transient eddies it is much more difficult to include the effects of the forced motion, which in turn depends upon the distribution of oceans and continents and the topography of the continents. The parameterizations as used here, or even more complicated forms, are ultimately undesirable in studies of the general circulation. However, studies of this type can be used to obtain a preliminary, empirical description of the axisymmetric flow and the major physical factors which determine the distribution of the various quantities as a function of time and latitude.

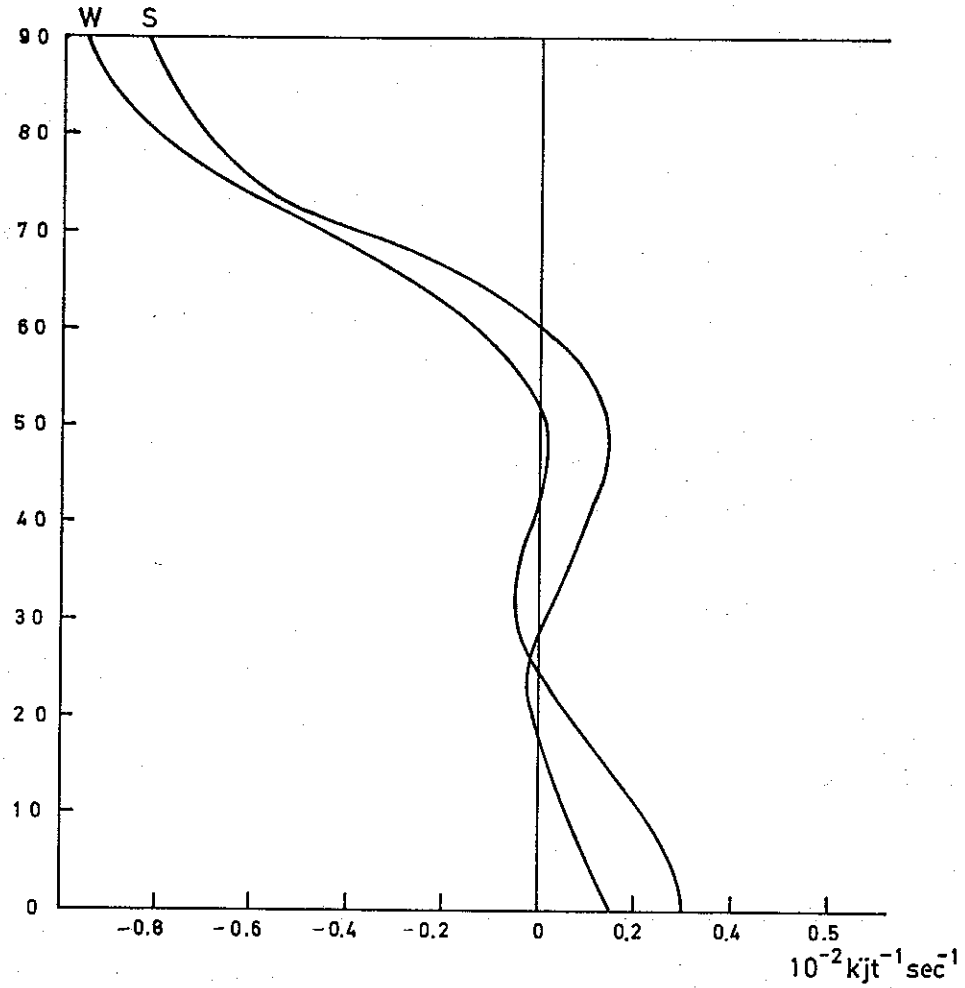

Fig. 16: The average heating for the winter and the summer season as a function of latitude for exp. No. 10. Unit: 10^{-2} kj t^{-1} sec^{-1}.

Acknowledgement. The present work would not have been possible without the excellent programming provided by Mr. James Pfaendtner, who not only did the programming of the basic model, but also the calculation of the derived quantities. The author would also like to thank Mr. Norman McFarlane for checking the complicated derivations used in this study.

This study has in part been supported by the National Science Foundation through Grant GA–16166 while the author was affiliated with the University of Michigan.

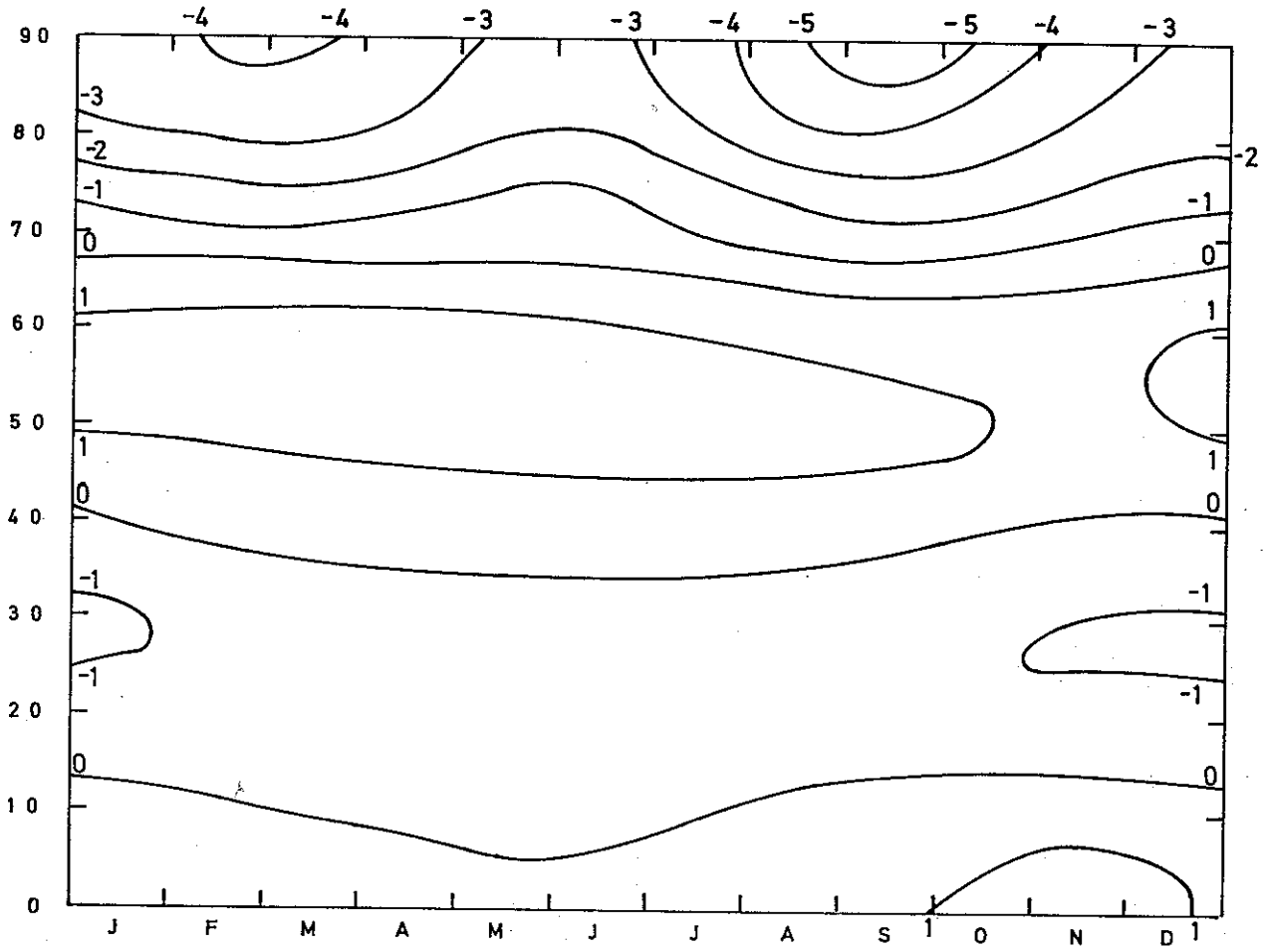

Fig. 17: The zonally averaged vertical velocity as a function of latitude and time for exp. No. 10. Unit: mm sec^{-1}.

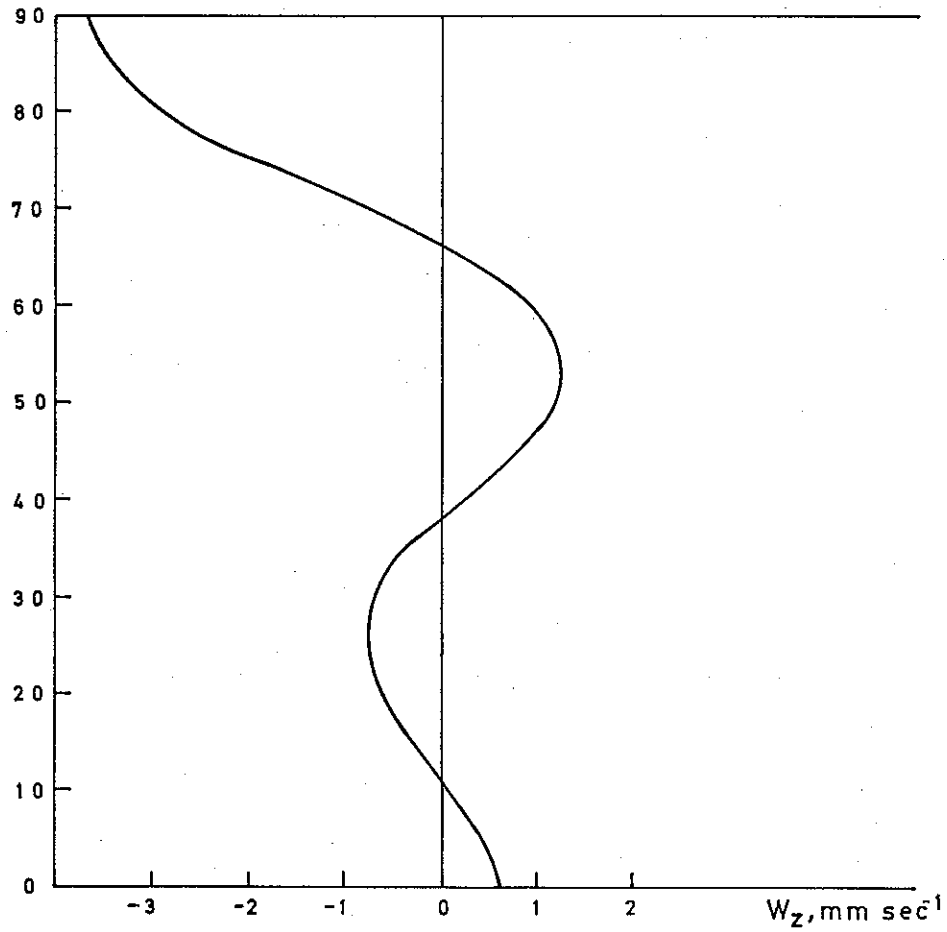

Fig. 18: Annual mean of the zonally averaged vertical velocity as a function of latitude for exp. No. 10. Unit: mm sec^{-1}.

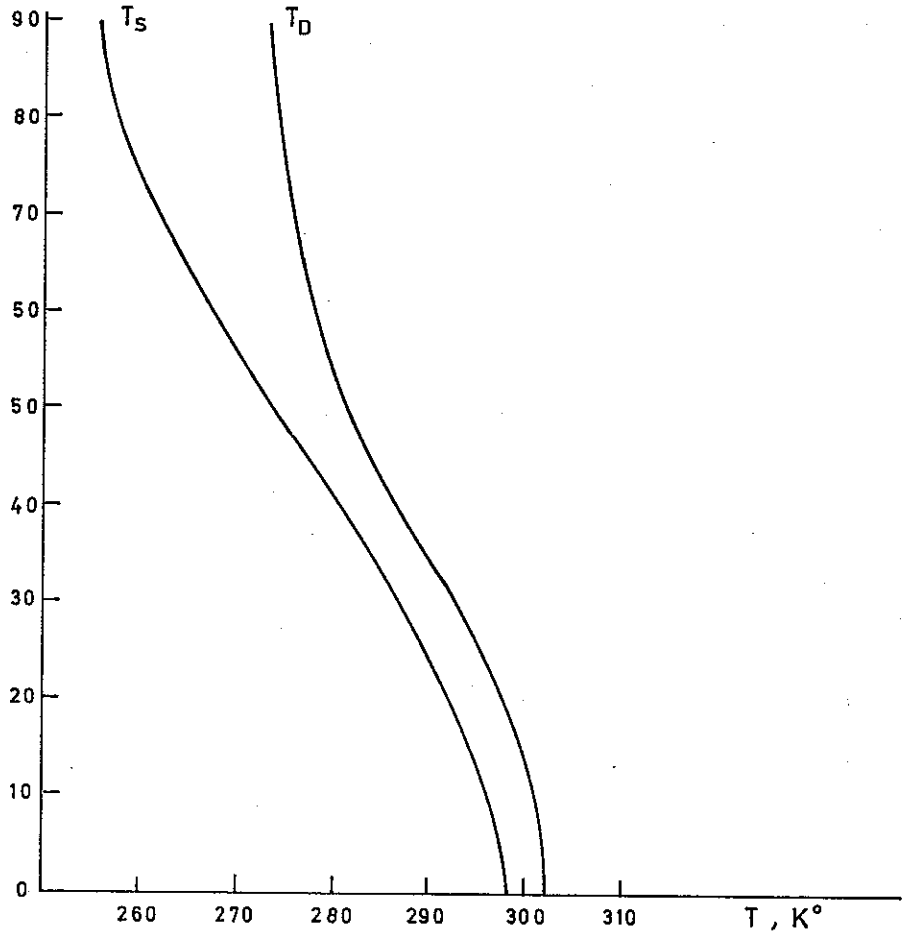

Fig. 19: The surface temperature T_s and the subsurface temperature T_D as a function of latitude in the average for the winter season as predicted in experiment No. 10.

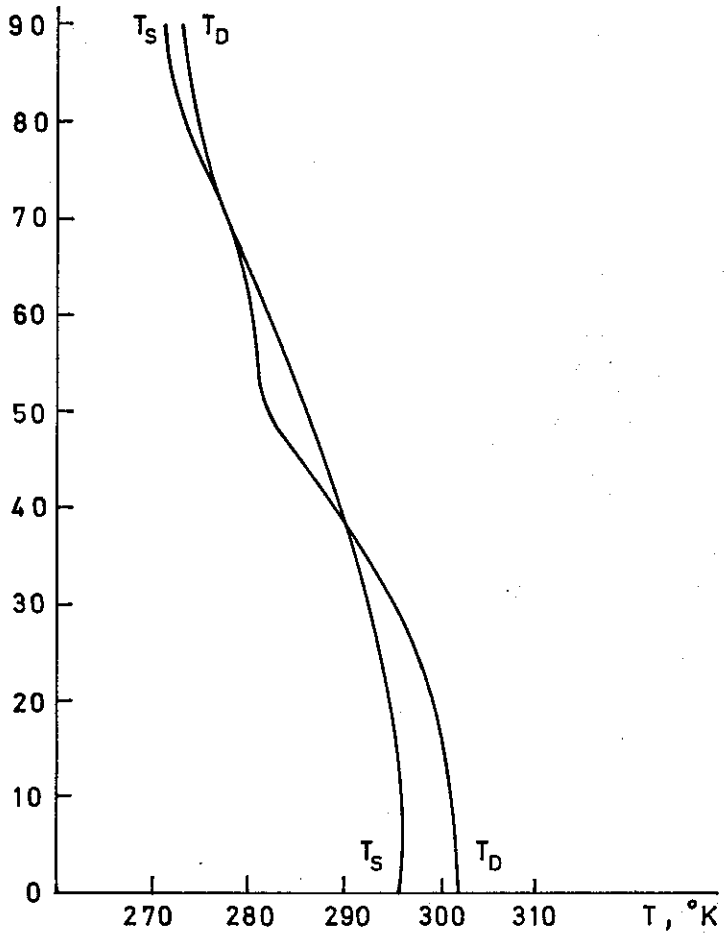

Fig. 20: As Fig. 19, but for the summer season in experiment No. 10.

References

Buch, H. S., 1954: Hemispheric wind conditions during the year 1950, Final Report, Part II, Contract AF 19(122)–153, Department of Meteorology, Massachusetts Institute of Technology.

Clark, N. E., 1967: Report on an investigation of large-scale heat transfer processes and fluctuations of sea-surface temperature in the North Pacific Ocean, Solar Energy Research Fund, Massachusetts Institute of Technology, 147 pp.

Crutcher, H. L., 1959: Upper Wind statistics charts of the northern hemisphere, Office of Chief of Naval Operations, Washington, D.C.

Crutcher, H. L., 1961: Meridional cross-sections. Upper winds over the northern hemisphere, Technical paper No. 41, US. Weather Bureau, Washington, D.C.

Green, J. S. A., 1970: Transfer properties of the large-scale eddies and the general circulation of the atmosphere, Quarterly Journal of the Royal Meteorological Society, Vol. 96, pp. 157–185.

Heastie, H. and P. M. Stephenson, 1960: Upper winds over the world, part I and II, Geophysical Memoirs No. 103, Meteorological Office, London, 217 pp.

Jenne, R. L., H. van Loon, J. J. Taljaard and H. L. Crutcher, 1968: Zonal means of climatological analyses of the southern hemisphere, Notos, Vol. 17, pp. 35–52.

Kraus, E. B. and E. N. Lorenz, 1966: Numerical experiments with large-scale seasonal forcing, Journal of Atmospheric Sciences, Vol. 23, pp. 3–12.

Kung, E. C. and S. T. Soong, 1969: The march of seasons in kinetic energy of the atmosphere, Quarterly Journal of the Royal Meteorological Society, Vol. 95, pp. 501–512.

Lorenz, E. N., 1967: The nature and theory of the general circulation of the atmosphere, World Meteorological Organization No. 208, TP 115, 161 pp.

Obasi, G. O. P., 1963: Poleward flux of atmospheric angular momentum in the southern hemisphere, Journal of Atmospheric Sciences, Vol. 20, pp. 516–628.

Palmén, E. and C. Newton, 1969: *Atmospheric Circulation Systems*, Academic Press, New York, 603 pp.

Peixoto, J. P., 1960: Hemispheric temperature conditions during the year 1950, Scientific Report No. 4, Contract AF 19(604)–6108, Dept. of Meteorology, Massachusetts Institute of Tecnology.

Saltzman, B. and A. Fleisher, 1961: Further statistics on the modes of release of available potential energy, Journal of Geophysical Research, Vol. 66, pp. 2271–2273.

Saltzman, B., 1968: Steady state solutions for the axially-symmetric climatic variables, Pure and Applied Geophysics, Vol. 69, pp. 237–259.

Sela, J. and A. Wiin-Nielsen, 1971: Simulation of the atmospheric annual energy cycle, Monthly Weather Review, Vol. 99, No. 6, pp. 460–468.

Sellers, W. D., 1966: *Physical Climatology*, University of Chicago Press, 272 pp.

Wiin-Nielsen, A., 1959: A study of energy conversion and meridional circulation for the large-scale motion in the atmosphere, Monthly Weather Review, Vol. 87, pp. 319–332.

Wiin-Nielsen, A., 1967: On the annual variation and spectral distribution of atmospheric energy, Tellus, Vol. 19, pp. 540–559.

Wiin-Nielsen, A., 1968 a: On atmospheric response to large-scale seasonal forcing, Proceedings of Symposium on Numerical Weather Forecasting, Tokyo, Japan, pp. IV–21–IV–27.

Wiin-Nielsen, A., 1968 b: On the intensity of the general circulation of the atmosphere, Reviews of Geophysics, Vol. 6, No. 4, pp. 559–579.

Wiin-Nielsen, A., 1970: A theoretical study of the annual variation of atmospheric energy, Tellus, Vol. 22, pp. 1–16.

Wiin-Nielsen, A., 1971: A simplified theory of the annual variation of the general circulation, Geophysica, Vol. 11, No. 2, pp. 165–184.

Wiin-Nielsen, A. and J. Sela, 1971: On the transport of quasigeostrophic potential vorticity, Monthly Weather Review, Vol. 99, No. 6, pp. 447–459.

APPENDIX 1

A series of experiments has been described in this paper as summarized in Tables V and VI. As the experiments have been arranged, it is evident that the last experiments are the most complete with respect to the physical processes incorporated in the model. It is of pedagogical interest to investigate the results of experiment No. 1 because this experiment considers radiational processes only and pays no attention to the effects of the eddies on the zonal current. Experiment No. 1 is therefore, in the usual context, the answer to the question: What kind of circulation will we get if we disregard the interaction between the eddies and the zonal current and consider only the axially symmetric circulation created by the radiational heating and modified by friction?

It is immediately obvious from Table V that we will get a circulation with a very large amount of zonal available potential energy during winter and an extremely small amount of this form of energy during summer. This means that the temperature contrast between pole and equator is very large during winter and small or even reversed during summer. On the other hand, it is also evident from Table V that a relatively small amount of kinetic energy is in existence in this experiment.

Since the exchange between the zonal average and the eddies is disregarded in exp. No. 1, it is obvious that $C(A_z, A_E) = C(K_E, K_z) = 0$. On the other hand, the generation of zonal available potential energy $G(A_z)$ is not very large, indicating a level quite comparable to those found in the other experiments. The main difference between exp. No. 1 and all the other experiments is that $C(A_z, K_z)$ and $D(K_z)$ are much larger because they represent the only other processes. We must therefore expect that the mean meridional circulation is arranged in such a way that a more efficient conversion $C(A_z, K_z)$ can take place. In order to illustrate this point we have prepared Fig. A1 and Fig. A2 which show that a single Hadley cell exists in the mean meridional circulation. As indicated by Fig. A2 the cell is thermally direct, and it is much more efficient than the mean meridional circulation presented in Fig. 17 and Fig. 18. In spite of the more efficient arrangement of the mean meridional circulation it is also indicated in Fig. A2 that this circulation cannot manage to provide a large meridional transport of heat as indicated by a comparison between the annual average of the temperature predicted in exp. No. 1 and the equilibrium temperature which would exist if there were no circulation.

It can be shown from (2.18) and (2.19) that the annual average of the zonal wind at the lower level (75 cb) is zero if we disregard the interaction between the zonal average and the eddies. This statement was verified by the actual calculation. On the other hand, it is possible to have a non-zero zonal wind at any time during the year. It is of interest to illustrate the distribution of the zonal winds in exp. No. 1. Fig. A3 shows the zonal winds during the winter season (October-March, incl.) at the upper and the lower levels computed from the results of exp. No. 1. The upper level (25 cb) has a broad band of strong westerlies, while the lower level (75 cb) has extremely weak easterlies. As illustrated in Fig. A4 the upper level westerlies are considerable weaker in summer than in winter, while the zonal winds at the lower level are weak westerlies.

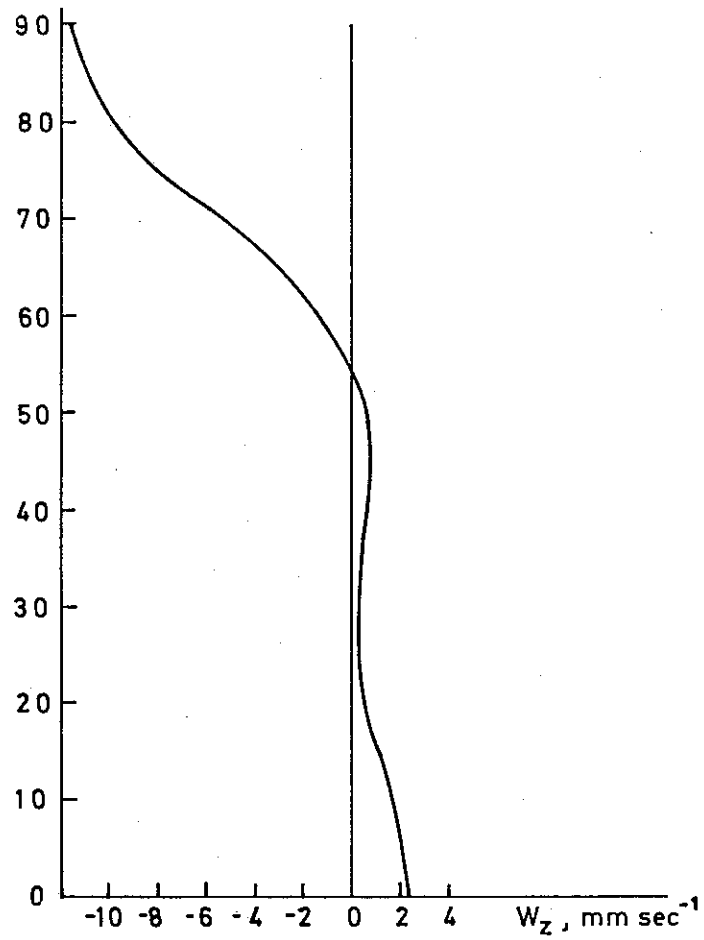

Fig. A1: Annual mean values of the zonally averaged vertical velocity in exp. No. 1. Unit: mm sec^{-1}.

A comparison between the figures in the appendix and the corresponding figures in the main text shows clearly the importance of the interaction between the eddies and the zonal average and the necessity to parameterize these processes in an accurate way.

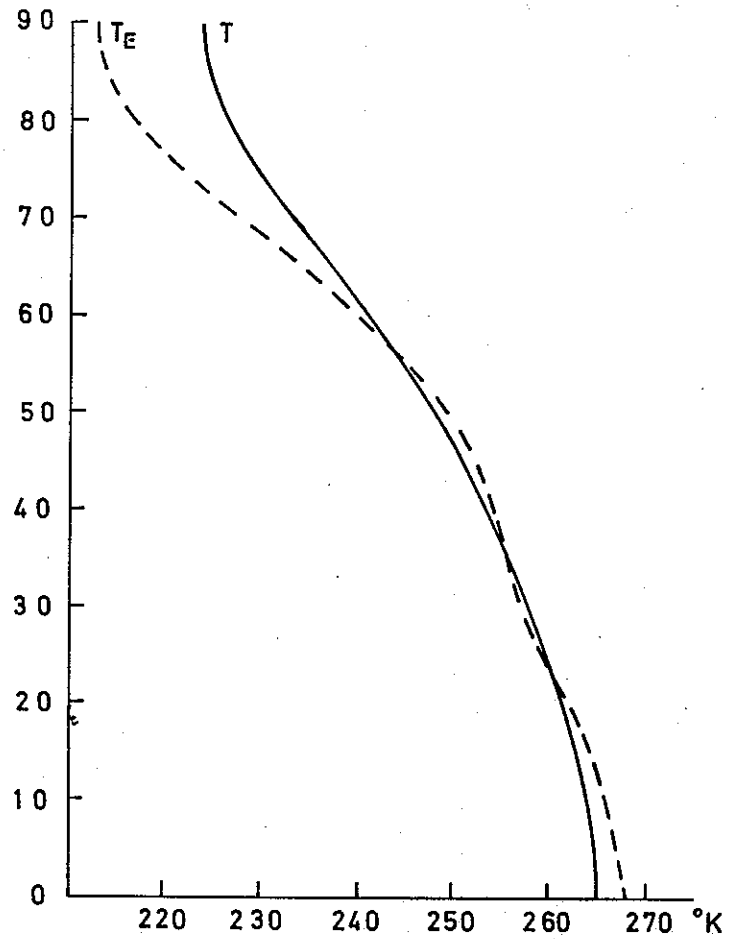

Fig. A2: The annual mean values of the zonally averaged temperature and equilibrium temperature in exp. No. 1. Unit: ^{0}K.

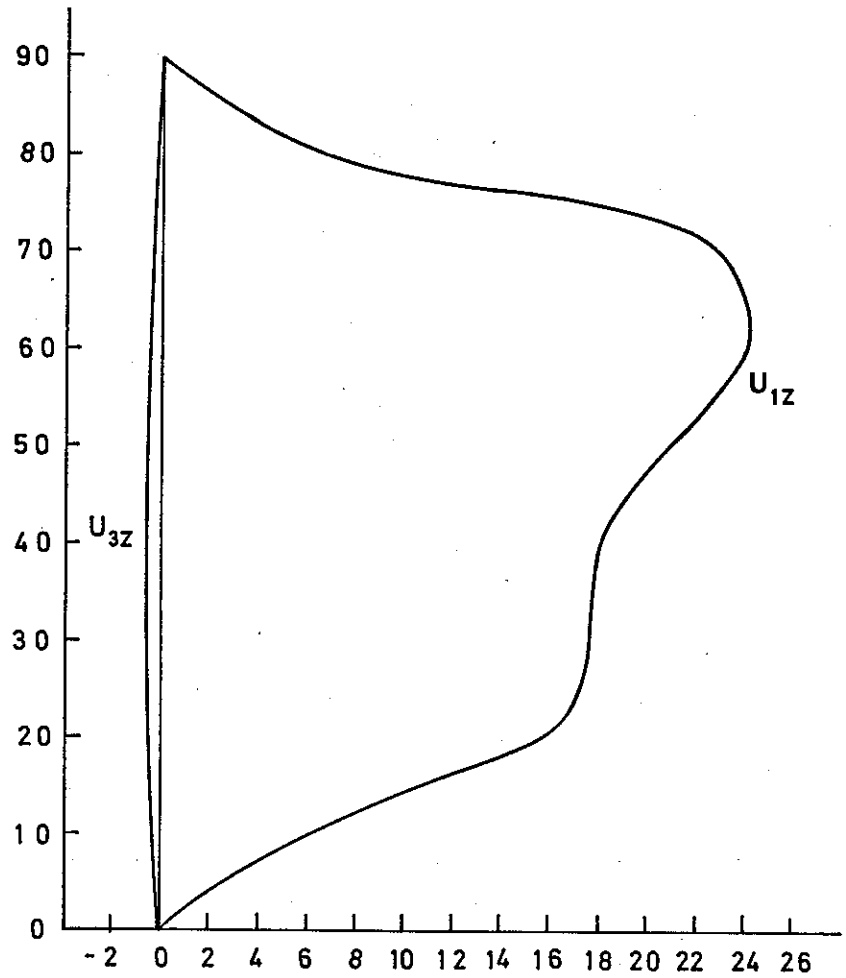

Fig. A3: The zonally averaged wind at the upper and the lower level for the winter season in exp. No. 1. Unit: m sec^{-1}.

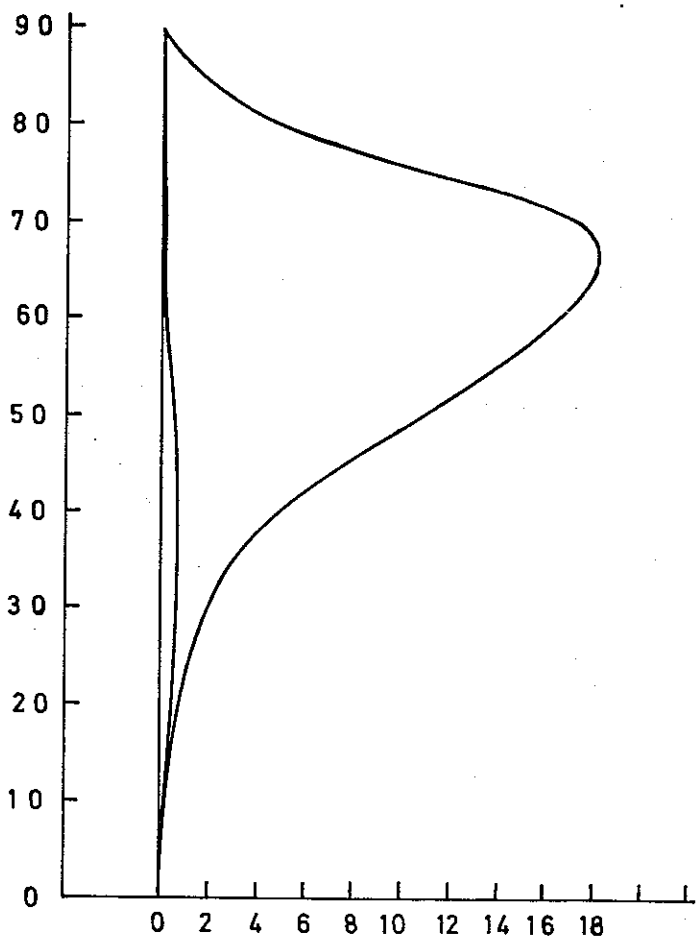

Fig. A4: As Fig. A3, but for the summer season.

APPENDIX 2

The heating function. The purpose of this appendix is to analyse some aspects of the heating function as employed in the present model. In the earlier attempts to simulate the annual variation of the zonally averaged state of the atmosphere we have employed a heating of a Newtonian form. The heating function in this model contains several other physical processes in the specification of the diabatic heating. It is therefore worth while to investigate the nature of the new heating mechanism.

The summary of various heating processes is given in Table I. Using (2.16) and the approximation (2.22) we may write

$$(1-x)(1-r_a)(1-r_s)R_o + N_1\sigma_B 4A^3T - \sigma_B 4A^3T_S - N_1\sigma_B 3A^4 + \sigma_B 3A^4$$

$$- b(T_s - T) - c + w[e\{-b(T_s - T) - c\} + f] - k(T_s - T_D) = 0 \quad (A1)$$

which expresses the heat balance at the ground. The net heat transfer to the atmospheric column is given by (2.15). Writing this expression in detail and using again (2.22) we get

$$HT_a = X(1-r_a)R_o + \sigma_B\Gamma 4A^3T_s - \sigma_B\Gamma 3A^4 - \sigma_B(N_1+N_2)4A^3T$$

$$+ \sigma_B(N_1+N_2)3A^4 + b(T_s - T) + c - \tfrac{1}{2}\int_{-1}^{+1} w\,[e\{-b(T_s - T) - c\} + f]d\mu \quad (A2)$$

We may now use (A1) and (A2) to define an equilibrium temperature T_E. This temperature will be the one which must exist if (A1) and $HT_a = 0$ are both to be satisfied. Because we have these two relations it is possible to eliminate one of the temperatures, in this case T_s, and we may then express T_E in terms of R_o and T_D. The details of these calculations will be given a little later, but let us assume that T_E has been determined. Subtracting the equation $HT_a = 0$ from HT_a as given in (A2) we may write the expression for the heating function in the form:

$$HT_a = -[(N_1+N_2)4\sigma_B A^3 + b](T - T_E) - \tfrac{1}{2}\,\mathrm{web}\int_{-1}^{+1}(T - T_E)d\mu \quad (A3)$$

If we require at any given point in time that the area mean of HT_a shall be zero, i.e. that the area mean over the whole globe of the atmospheric temperature is constant, then it follows from (A3) that

$$\int_{-1}^{+1}(T - T_E)d\mu = 0 \quad (A4)$$

and the heat transfer takes the form

$$HT_a = -[(N_1 + N_2)4\sigma_B A^3 + b](T - T_E) \tag{A5}$$

It is seen from (A5) that the heating, even in this general case, is of a Newtonian form, and that it is possible to calculate the coefficient in (A5) from the numerical values. The main difference between (A5) and the previous forms of Newtonian heating is then the calculation of the equilibrium temperature and the coefficient.

Using the formulation considered in the numerical experiments we find for the coefficient as considered by Wiin-Nielsen (1970) and Sela and Wiin-Nielsen (1971), i.e.

$$H_2 = -\gamma Cp(T - T_E) \tag{A6}$$

that

$$\gamma = \frac{1}{C_p}\frac{g}{p_o}[(N_1 + N_2)4\sigma_B A^3 + b] \tag{A7}$$

Adopting the numerical values as used in the most advanced experiments in this series we find that

$$\gamma = 1.4 \times 10^{-6}\ \text{sec}^{-1}$$

If we, on the other hand, restrict ourselves to a case of radiational equilibrium we find

$$\gamma = 1.0 \times 10^{-6}\ \text{sec}^{-1}$$

These values are of the same order of magnitude, although slightly larger, than those used earlier. We mention in addition that the heating intensity is determined not only by the coefficient γ, but naturally also by the field T_E, and this field changes each time a new process is introduced.

In order to find an expression for the equilibrium temperature we solve (A1) for T_s because we want to eliminate this variable. Denoting

$$\begin{aligned} N &= k + 4\sigma_B A^3 + b(1 + eu) \\ C_1(R_o) &= (1 - X)(1 - r_s)(1 - r_a) \\ C_1(T_E) &= N_1 \cdot 4\sigma_B A^3 + b(1 + eu) \\ C_1(T_D) &= k \\ C_1(0) &= wf - wec - c - (N_1 - 1)3\sigma_B A^4 \end{aligned} \tag{A8}$$

we may write

$$T_s = N^{-1}(C_1(R_o)R_o + C_1(T_E)T_E + C_1(T_D)T_D + C_1(0)) \tag{A9}$$

We turn next to the equation

$$HT_a = 0, \text{ when } T = T_E$$

Denoting here

$$\begin{aligned} C_2(R_o) &= X(1 - r_a) \\ C_2(T_s) &= \Gamma 4\sigma_B A^3 + b \\ C_2(T_E) &= -[(N_1 + N_2)4\sigma_B A^3 + b] \\ C_2(0) &= -\Gamma 3\sigma_B A^4 + (N_1 + N_2)3\sigma_B A^4 + c + wec - wf \end{aligned}$$

we may write (A10) in the form

$$C_2(R_o)R_o + C_2(T_s)T_s + C_2(T_E)T_E + C_2(0) + \tfrac{1}{2}\, web \int_{-1}^{+1} (T_s - T_E)\, d\mu = 0 \qquad \text{(A11)}$$

Substituting from (A9) in (A11) we find:

$$\begin{aligned} &[C_2(R_o) + N^{-1}C_2(T_s)C_1(R_o)]R_o \\ &+ [C_2(T_E) + N^{-1}C_2(T_s)C_1(T_E)]T_E + N^{-1}C_2(T_s)C_1(T_D)T_D \\ &+ [C_2(0) + N^{-1}\, C_2(T_s)C_1(0)] + \tfrac{1}{2} web \int_{-1}^{+1} (T_s - T_E)\, d\mu = 0 \end{aligned} \qquad \text{(A12)}$$

It would be a straight forward matter to determine T_E in terms of R_o and T_D if it were not for the last integral in (A12). It is therefore necessary to determine first the integral

$$I(T_E) = \int_{-1}^{+1} T_E\, d\mu \qquad \text{(A13)}$$

This is done by integrating (A12) from -1 to $+1$ with respect to μ. Using the notation introduced in (A13) for the other variables too we find from (A12) that

$$\begin{aligned} &(C_2(T_E) + N^{-1}C_2(T_s)C_1(T_E) + web(N^{-1}C_1(T_E) - 1)]I(T_E) \\ &+ [C_2(R_o) + N^{-1}C_2(T_s)C_1(R_o) + web\, N^{-1}C_1(R_o)]I(R_o) \\ &+ [N^{-1}C_2(T_s)C_1(T_D) + web\, N^{-1}C_1(T_D)]I(T_D) \\ &+ 2[C_2(0) + N^{-1}C_2(T_s)C_1(0) + web\, N^{-1}C_1(0)] = 0 \end{aligned} \qquad \text{(A14)}$$

(A14) can be used to calculate $I(T_E)$since the equation is linear. Having this information we may now return to (A12) and determine the local values of T_E from the equation:

$$\begin{aligned} &[C_2(T_E) + N^{-1}C_2(T_s)C_1(T_E)]T_E \\ &+ [C_2(R_o) + N^{-1}C_2(T_s)C_1(R_o)]R_o + N^{-1}C_2(T_s)C_1(T_D)T_D \\ &+ [C_2(0) + N^{-1}C_2(T_s)C_1(0)] + \tfrac{1}{2}\, web\, N^{-1}C_1(R_o)I(R_o) \\ &+ \tfrac{1}{2}\, web(N^{-1}C_1(T_E) - 1)I(T_E) + \tfrac{1}{2}\, web\, N^{-1}C_1(T_D)I(T_D) + web\, N^{-1}C_1(0) = 0 \end{aligned} \qquad \text{(A15)}$$

The procedure outlined above has been used to calculate $T_E = T_E(\mu)$ for the various cases.